Kinase Chemogenomics: Targeting the Human Kinome for Target Validation and Drug Discovery

E. ter Haar, W.P. Walters, S. Pazhanisamy, P. Taslimi, A.C. Pierce, G. W. Bemis, F.G. Salituro and S.L. Harbeson*

Vertex Pharmaceuticals, Inc., 130 Waverly Street, Cambridge, Massachusetts 02139, USA

Abstract: Chemogenomics is a gene family-based approach to drug discovery and target validation. This review will summarize the application of this interdisciplinary approach to the protein kinases of the human genome with emphasis upon the synergies and efficiencies to be gained. Specific examples from the SAPK-family will be discussed.

Keywords: Chemogenomics; kinases; structure-based drug design; VX-745; p38; JNK; REOS; virtual screening

INTRODUCTION TO CHEMOGENOMICS

The sequencing of the human genome [1,2] has produced a wealth of genomic information, which the pharmaceutical and biotechnology industries are capitalizing on in their research efforts towards the discovery of important new drugs. The approximately 30,000 genes found (less than the 100,000 or so anticipated genes) represent a large number of potential targets. As others have noted, a majority of these genes will not be appropriate drug targets [3]; therefore, the research community has to organize their efforts such that target validation and drug discovery proceed in a complementary fashion. Chemogenomics represents a parallel approach to target validation and drug discovery. In this review, we will discuss chemogenomics as it has been applied to the kinome – the protein kinases of the human genome [4].

Chemogenomics can be defined as the discovery and description of all possible drugs to all possible drug targets [5]. The aim of chemogenomics is to apply the modern tools and techniques of the drug discovery process in parallel to gene families. In this way, the efficiency-enhancing tools of modern drug discovery, such as high-throughput screening (HTS), high-throughput synthesis, structure-based drug design, *in vitro* biological assays, *in vivo* models, and modern computational methods, are leveraged across multiple targets within a gene family. A chemogenomic approach to drug discovery exploits the technical and informational synergies gained from targeting related members of a gene family, thereby providing relevant information in parallel rather than through a slower, iterative process. Although the pharmaceutical industry has traditionally organized its research along therapeutic areas, chemogenomics offers an alternative and complementary approach, since targets within a gene family can provide access to mechanistic pathways involved in a range of disease states. As noted previously [5], a disease indication focus divides biological and chemical expertise across therapeutic areas and does not exploit the synergies gained from targeting closely related active sites. Although some *in vitro* and *in vivo* testing will be applicable to specific therapeutic areas, other techniques such as HTS, expression profiling, cell assays, physical properties measurements, and proteome profiling may have kinome-wide applications that provide tools and information that benefit the discovery process for multiple targets.

In a chemogenomic approach to kinases, ATP site-directed inhibitors are valuable reagents that are used across the gene family. The greatest value to the discovery of new inhibitor leads is realized when a kinase inhibitor collection is tested across kinases irrespective of the therapeutic indication. The compounds are ideally diverse, drug-like molecules representing many kinase inhibitor scaffolds with sufficient representation within a scaffold class to allow SAR to emerge directly from the screen. When screening identifies leads for a new target, these leads will require optimization of potency and selectivity but should already possess drug-like physical properties. This allows medicinal chemistry to focus more on improving activity and selectivity versus the target rather than solubility and chemical stability. The optimized leads can then be used for target validation as small molecule "chemical knockouts" in disease models. If validation is successful, medicinal chemistry then further optimizes the lead to provide a preclinical candidate. As will be discussed later, this methodology presents a challenge in information management.

Kinases are ideally suited to a gene family approach to drug discovery. A recent review by Manning proposes that the human genome codes for 518 protein kinase genes, which represents approximately 1.7% of the human genes [4]. Comparison of the kinase chromosomal map with a map of known disease loci reveals that 244 kinases map to disease loci [6]. It is unlikely that all of these kinases will be therapeutic targets; however, the recent increase of kinase-targeted drugs in development suggests a substantial number will be successful [7,8]. A review by Hopkins proposes that of the approximate 30,000 genes in the human genome, only 10-14% of these represent targets that have a high probability of binding small molecules and of these, only 600-1500 genes will be therapeutically relevant targets [3]. If Hopkins is correct, and kinases make up approximately 22% of the proteins that can be targeted with small molecules,

*Address correspondence to this author at the Vertex Pharmaceuticals, Inc., Department of Medicinal Chemistry, 130 Waverly Street, Cambridge, MA 02139, USA; E-mail: Harbeson@vpharm.com

1389-5575/04 $45.00+.00

then the number of therapeutically relevant kinases would be in the range of 130-300. This is an attractive number of new therapeutic targets from a gene family. These observations show the potential for a chemogenomic approach to kinase-targeted drug discovery and this potential is currently being exploited in the industry as exemplified by the investment of Novartis Pharmaceuticals in the chemogenomic research platform of Vertex Pharmaceuticals, Inc.

This article will review the implementation of a chemogenomic research plan directed toward the human kinome. To fully realize the benefits of kinase chemogenomics, all stages of research should be structured to apply common information and reagents across the gene family. Within the chemogenomic program at Vertex, kinase structure, HTS, enzymology, computational chemistry, library design, medicinal chemistry, and information management have all been engineered to fully maximize the synergies. The final section of the review will focus on specific examples of the successful application of chemogenomics to the SAPKs (Stress Activated Protein Kinases).

STRUCTURAL BASIS FOR CHEMOGENOMICS: THE ATP-BINDING SITE

The earliest X-ray studies of kinases characterized the three-dimensional structure of the catalytic domain [9,10]. The structure of cAMP-dependent protein kinase [PKA] was the first protein kinase solved by X-ray crystallography [11,12]. As more X-ray structures of kinases were solved, it became apparent that Ser/Thr kinases share structural similarity not only with each other but also with Tyr kinases [13-15]. The relative similarity -- coupled with subtle differences that can be exploited for selectivity -- make kinase ATP-binding sites ideal targets for reuse of the three dimensional structural knowledge across multiple kinase targets. This provides a sound foundation to a chemogenomic-based approach to drug discovery.

The recently published crystal structure of GSK-3β shown in Fig. (**1**) is a prototypical example of kinase domain structure [16]. The kinase domain of GSK-3β is approximately 300 residues long and folded in two lobes.

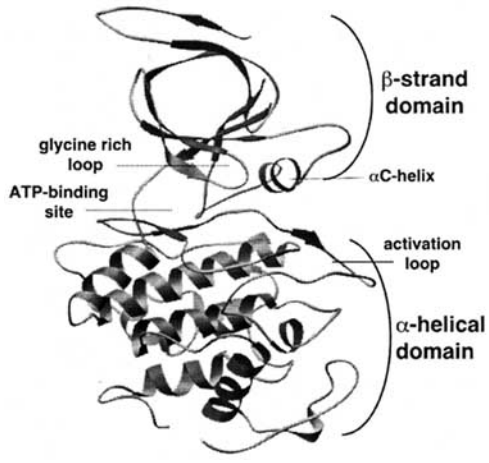

Fig. (1). Crystal structure of the Ser/Thr kinase, GSK-3β [16].

The N-terminal lobe contains five β-strands and one α-helix, whereas the C-terminal lobe contains mainly α-helices. ATP binds in a deep cleft at the interface of the two lobes. The substrate is held in place in front of the ATP-binding site by the activation loop that is approximately 25 residues long. When this site is occupied with ATP and the substrate-binding groove with a target substrate, the kinase domain catalyzes the transfer of the ATP γ-phosphate to the substrate.

Sequence alignments for various kinases (Fig. (**2b**)) show that there are significant sequence variations in the residues of the ATP-binding site that are not involved in phosphate transfer. The structure of AMPPNP bound to CDK2 in Fig. (**3a**) shows that ATP does not occupy all the available pockets of an ATP-binding site [17]. The ATP-binding site can be divided into different sections that contribute to inhibitor potency or specificity: phosphate transfer area, glycine rich loop, upper hinge region, lower hinge region, and a hydrophobic pocket that is indicated in Fig. (**3a)** and Fig. (**3b**). The residues involved in the γ-phosphate transfer are conserved among kinases – positions 4 and 19-20 in Fig. (**2a**). They cluster around the three phosphates of ATP and are important for optimal phosphate transfer. The catalytic residues align the α-helical and β-strand domains and align the γ-phosphate with the target residue. These residues are typically not targeted in inhibitor design, although contacts can contribute to the potency of the inhibitor.

The glycine rich loop Fig. (**1**) acts as a lid on the ATP-binding site. It is a flexible anti-parallel β-sheet that adjusts its conformation to the molecule occupying the ATP-binding site. The sequence of the glycine rich loop is fairly conserved with three glycines, two hydrophobic residues that point into the ATP-binding site and one bulky hydrophobic residue at the tip of the loop. The side-chain of the latter may be pulled into the ATP-binding site depending on the type of molecule present. The two hydrophobic residues that point into the ATP-binding site contribute to and help define the hydrophobic environment of the ATP-binding site – positions 1 and 2 in Fig. (**2a**). This leads to the general conclusion that the glycine rich loop contributes more to the potency of the inhibitor than to the specificity.

The hinge region connecting the α-helical and β-strand domains allows the two domains to rotate with respect to each other – positions 10-16 in Fig. (**2a**). As shown in Fig. (**2b**), there is little homology between hinge residues of different kinases; however, the adenine portion of ATP makes the same hydrogen bonds to the hinge residues in all kinases: N6 donates a hydrogen to a backbone carbonyl of a hinge residue X and N1 accepts a hydrogen from the amide nitrogen of residue X+2. Inhibitors in the ATP-binding site uniformly hydrogen bond with one or more hinge residues. The residue side-chains rarely interfere with inhibitor binding.

One of the important sequence variations found in the ATP-binding site is the hydrophobic pocket that is formed by residues 4, 5, 7, 8, 9, and 18 in Fig. (**2a**). This is a deeply buried portion of the ATP-binding site that is not accessed by ATP itself but is often targeted by inhibitors to aid selectivity. Fig. (**3b**) shows how VK19911 (structure shown in Fig. (**4**)) makes such interactions with p38α [18].

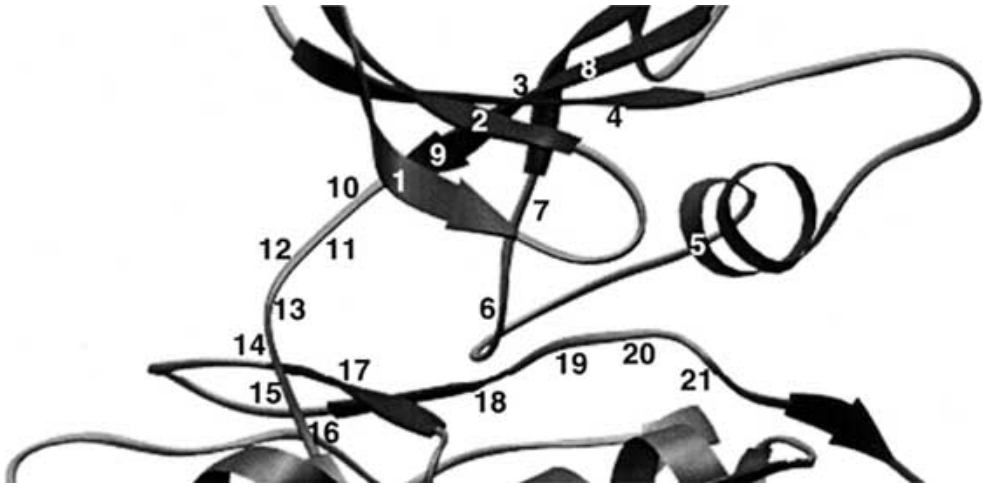

(a)

	1	2	3	4	5	6	7	8	9	10	11	12	13	14	15	16	17	18	19	20	21
INSR	L	V	A	K	M	V	L	V	M	E	L	M	A	H	G	D	M	G	D	F	G
IGF1R	.	.	.	.	.	.	.	.	.	.	.	.	T	R	.	.	.	.	.	.	.
EGFR	.	.	.	.	.	C	.	L	T	Q	.	.	P	F	.	C	L	T	.	.	.
FGFR	.	.	.	.	.	I	.	.	V	.	Y	A	S	K	.	N	L	A	.	.	.
Ephb2R	I	.	.	.	.	I	.	I	T	.	F	.	E	N	.	S	L	S	.	.	.
SRC	.	.	.	.	.	.	.	I	T	.	Y	.	S	K	.	S	L	A	.	.	.
ABL	.	.	.	.	.	.	.	I	T	.	F	.	T	Y	.	N	L	A	.	.	.
HCK	.	.	.	.	.	.	.	I	T	.	F	.	.	K	.	S	L	A	.	.	.
BTK	.	.	.	.	.	.	.	I	T	.	Y	.	.	N	.	C	L	S	.	.	.
CSK	I	.	.	.	.	.	.	I	T	.	Y	.	.	K	.	S	L	S	.	.	.
p38	V	.	.	.	L	I	.	L	T	H	.	.	G	A		.	A	L	.	.	.
ERK2	I	.	.	.	L	I	I	I	Q	D	.	.	E	T		.	L	C	.	.	.
JNK3	I	.	.	.	.	I	.	L	.	.	.	.	D	A		N	V	L	.	.	.
CDK2	I	.	.	.	L	.	.	L	F	.	F	L	H	Q		.	L	A	.	.	.
GSK3B	I	.	.	.	.	.	.	L	L	D	Y	V	P	E		T	L	C	.	.	.

(b)

Fig. (2). (**a**). ATP-site of GSK-3β [16]. The numbers indicate the residues that affect ligand binding in the ATP-binding site. Residues 1,2,3,6,10-17 form the adenine binding pocket, residues 4,5,7,8,9,18 form the hydrophobic pocket, and residues 19-21 are conserved catalytic residues. (**b**). Sequence alignment of the ATP-binding residues of receptor tyrosine kinases: INSR [88], IGF1R [89], EGFR [90], FGFR [91], Ephb2R [92], non-receptor tyrosine kinases: SRC [93], ABL [24], HCK [94], BTK [95], CSK [96] and serine/threonine kinases: p38α [97], ERK2 [20], JNK3 [98], CDK2 [17], GSK-3β [16]. The crystal structures of the kinases were superimposed on INSR and the homologous residues were determined by visible inspection. Residues identical to the INSR sequence are indicated with a dot.

The selectivity profile of inhibitors can often be explained thorough sequence analysis of this site and use of the site can be crucial in the design of selective inhibitors. This will be discussed in greater detail later in the review where the design of selective p38α inhibitors is used as an example.

The ribose group of ATP will sometimes hydrogen-bond to hinge residue 16 in Fig. (**2a**) through one of its hydroxyl substituents [17,19]. This contact is not necessarily required for binding, since the sequence in this part of the ATP-binding site is not conserved among kinases Fig. (**2b**). The lower hinge portion, together with the glycine rich loop, form the opening of the ATP-binding site. Approximately 60% of the kinases have an additional glycine inserted at position 15 of the hinge Fig. (**2a-b**) resulting in a narrowing of the ATP-binding site opening, which can be used to improve the selectivity of an inhibitor class. Extending the inhibitor toward the glycine insertion may prevent the inhibitor from affecting a kinase that contains the insertion. Extending the inhibitor toward the opening of the ATP-

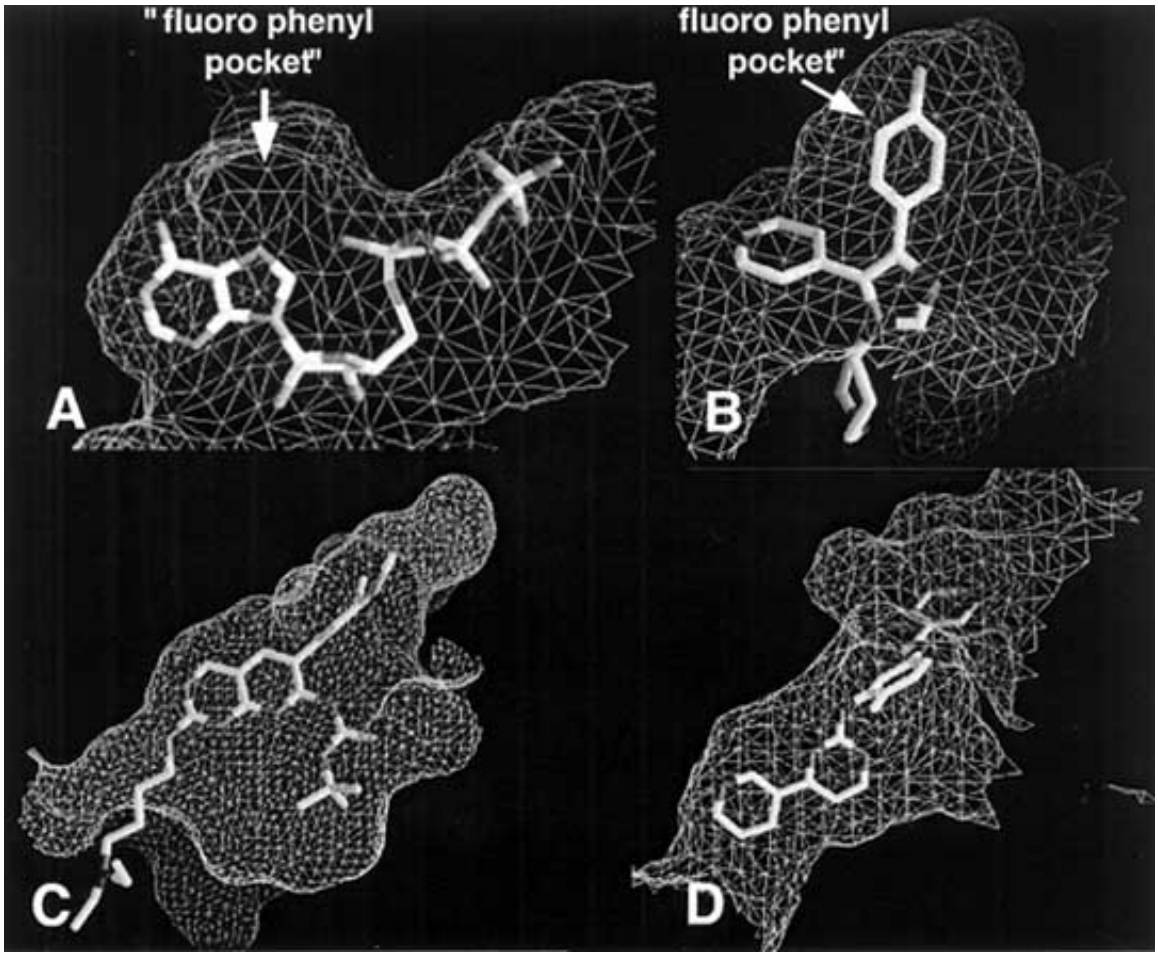

Fig. (3). Positioning of different ligands in the ATP-binding sites of four different kinases. **(a)** CDK2 in complex with AMPPNP [17]; **(b)** p38α in complex with VK19911 [18]; **(c)** FGF-receptor in complex with PD 173074 [91]; and **(d)** Abl in complex with STI-571 [24]. The location of the hydrophobic pocket is indicated.

binding site can also provide an effective strategy for improving the physical properties of compounds through the introduction of solubilizing groups.

In many kinases, the conformation of the activation loop (Fig. (**1**)) is dependent on the phosphorylation-state of this loop. In the inactive, non-phosphorylated form, the activation loop blocks the substrate-binding groove and the ATP-binding site, whereas in the active, phosphorylated state, the loop does not block the ATP-binding site or substrate-binding groove. In serine/threonine kinases, such as ERK and p38, the activation loop packs against the α-helical domain, and the phosphorylated threonine binds positive charged residues from the N- and C-terminal domains. These conformational changes lead to proper alignment of the two domains [20,21].

In Src-family kinases, the activation loop resides over the substrate-binding groove. In the non-phosphorylated state, the activation loop binds the α-C helix and blocks catalysis [22]. Upon phosphorylation, the activation loop releases the α-C helix and the phosphorylated residue binds two arginines that would otherwise block the substrate-binding groove. The large shifts that the activation loops undergo upon phosphorylation and activation of kinases have structural consequences for the ATP-binding sites. The N-terminal region of the activation loop (the DFG motif) is sometimes in close proximity to an inhibitor and a repositioning of these residues can block inhibitor binding. PD 173074 (Fig. (**4**)), shown in Fig. (**3c**) in complex with FGF receptor, is a potent inhibitor of the FGF receptor kinase but does not inhibit the insulin receptor kinase [23]. Superposition of the two kinase domains reveals that the difference in the position of the DFG motif is one of the reasons PD 173074 does not bind the insulin receptor. The repositioning of the activation loop is also the reason why STI-571 (Fig. (**4**)), which is shown in Fig. (**3d**) in complex with Abl, only binds to the inactive and unphosphorylated form of Abl [24]. The inactive form of Abl is unique compared to other tyrosine kinases, which explains the selectivity of the compound [25].

In structure-based drug design programs, the crystal structure of the target facilitates the optimization of inhibitor

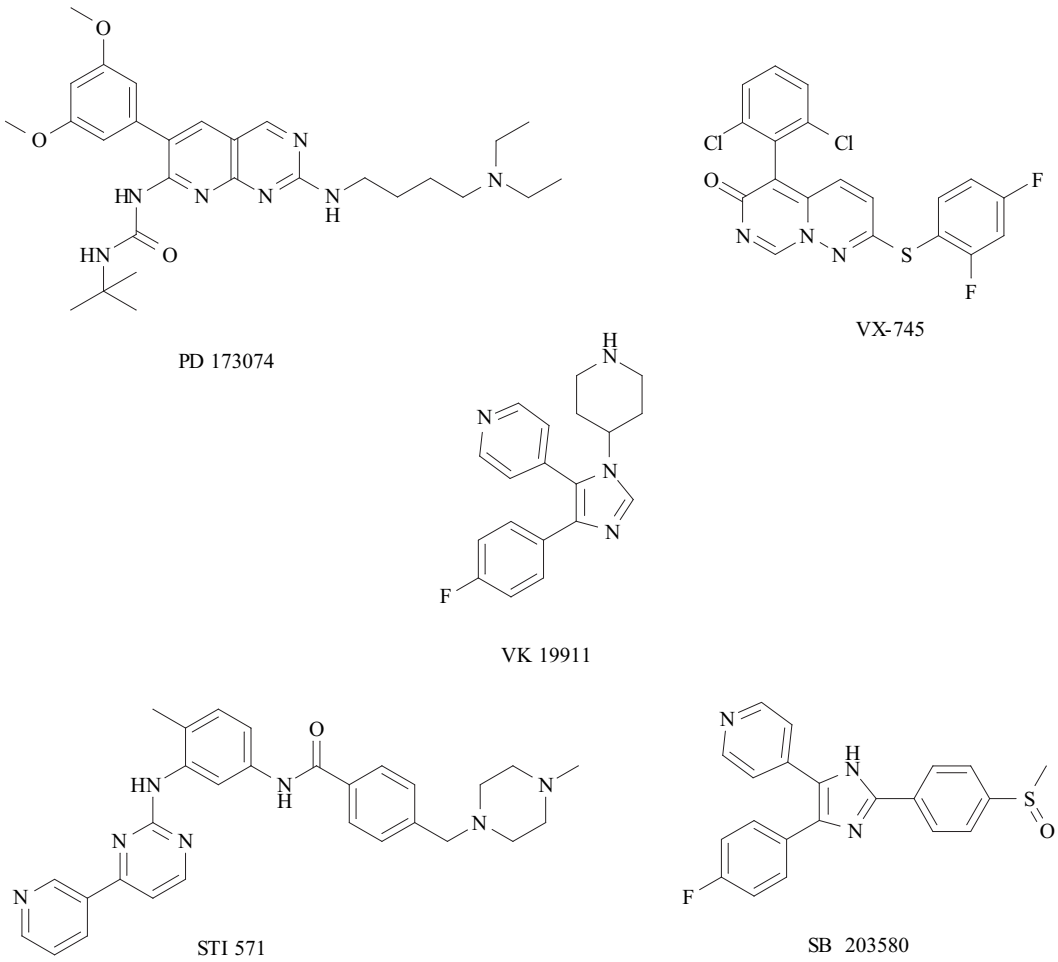

Fig. (4). Selected kinase inhibitors: PD 173074; STI-571; VX-745; SB-203580; and VK 19911.

potency and selectivity by defining key protein-inhibitor contacts. In chemogenomics, a family of structurally related proteins (such as kinases) is targeted and parallel drug design efforts are supported by multiple crystal structures from related proteins. For kinases, the ATP-binding site is targeted for inhibitor binding, which allows structure-activity relationships and specificity to be understood for each target kinase. This means that kinase targets without crystal structures can still benefit from structural knowledge gained from crystallographic studies of related kinases.

BUILDING THE KINASE COMPOUND COLLECTION

Due to the similarity of the ATP-binding sites, a collection of ATP-competitive inhibitor scaffolds should have broad utility across the gene family. This collection of compounds can provide the screening hits and medicinal chemistry leads to be used for structural analysis and kinase target validation. Chemogenomics requires that both the identification of hits and the hit to lead optimization process are tightly integrated with enzymology, cell biology, pharmacology, structural biology, and pharmacokinetics [26-28]. A hit inhibits kinase activity in a primary screen and is confirmed in a rigorous follow-up process. A lead is developed from a hit that has been chosen for optimization with a specific target. Lead optimization usually focuses on improving potency, selectivity, and PK properties. Optimized inhibitors can then be used for target validation. In chemogenomics, lead optimization occurs in parallel for multiple kinases and multiple inhibitor scaffolds. The compound collection is continuously enriched with drug-like molecules that have been optimized for improved potency and selectivity, and therefore, have a set of existing SAR vs. a number of kinases. This collection of kinase inhibitors has a much greater likelihood of producing leads directly from screening, and these leads may require minimal optimization prior to target validation in the appropriate *in vitro* assays or *in vivo* models.

HTS of small molecules against potential drug targets has become popular for lead discovery [29,30]. The quality of the compounds identified by screening, however, is dependent upon the quality of the screening library. The compounds used in HTS are usually from multiple sources such as in-house historical compounds, purchased commercial and private compounds, and combinatorial libraries. The age of historical archive collections within the pharmaceutical industry can be measured in decades, which makes the integrity of these compounds highly suspicious. These archive collections may be heavily populated with scaffolds that are not optimum for targeting kinases, such as beta-lactams, steroids, and glycosides, which would provide few if any useful hits for kinases. In the past, the acquisition

and library generation process has been driven by a need to increase the size and the "diversity" of compound collections [31], which was assumed to lead to greater success in HTS [30]. For chemogenomics, building the compound collection must place a high value on quality, since the leads obtained from HTS will be used for the validation of kinases as therapeutic targets. The chemical scaffolds represented within the collection must also be diverse yet retain those structural features consistent with targeting the ATP-binding site. Compound identity, integrity, and drug-likeness in conjunction with scaffold design must drive the implementation, maintenance, and expansion of the kinase screening collection.

Computational Tools

"Drug-like" is a popular term that has been reviewed by several authors [32-34]. Although definitions vary, the term drug-like refers to "molecules that contain functional groups and/or have physical properties consistent with the majority of known drugs" [32]. Evidence that compound collections can and do move towards non-drug-like properties has been clearly shown by the work of Lipinski in an analysis of the Pfizer compounds synthesized between 1984 and 1994 [35]. These researchers found that compound properties, such as molecular weight, numbers of hydrogen bond donors, acceptors, and rotatable bonds increased over the 10-year period. These observations, along with an analysis of known drugs, led to the proposed "rule of 5", which is a set of guidelines to determine whether or not a compound will be orally bioavailable. A majority of known orally bioavailable drugs follow these rules: hydrogen bond donors $\leq$5; hydrogen bond acceptors $\leq$10; molecular weight $\leq$500; and logP $\leq$5. Combinatorial libraries and compound collections elaborated before the generalized concept of drug-like and the "rule of 5" generally were directed towards maximum diversity and size with little effort to exclude those compounds that are not drug-like. HTS efforts are now directed to the discovery of leads that can be quickly brought forward for optimization rather than the simple identification of hits [36]. For chemogenomics, the identification of drug-like leads is a key to shortening the optimization process and providing tools for validation of kinases as relevant therapeutic targets.

In all cases, screening compounds should be chosen for their drug-like properties; therefore, one needs to apply "rules" or "filters" to identify the drug-like molecules. As discussed above, one set of filters that can be applied is the "rule of 5"; however, in an attempt to enhance the filters, researchers at Vertex Pharmaceuticals have developed the REOS (Rapid Elimination Of Swill) program [32,33,37]. This program not only expands upon the property filters but also adds a set of functional group filters that can be applied, which allows the removal of compounds containing reactive and/or undesirable functionality. In our experience, REOS removes 50-75% of the compounds in a typical commercial or combinatorial library [33]. Following a REOS analysis, a number of other computational techniques can be utilized to enrich a screening library with compounds having a high probability of becoming leads.

When protein crystal structures or homology models are available, computational docking techniques can be used to prioritize compounds for purchase or synthesis. A docking program evaluates thousands of orientations of each small molecule in a model of a protein active site [38]. A "scoring function" is then used to evaluate the complementarity of the small molecule and the active site [39]. One limitation of docking programs is the lack of accuracy in scoring functions used to predict binding affinity. One method of addressing these limitations is to employ a consensus approach that utilizes multiple scoring functions. A 1999 paper by Charifson and coworkers [40] describes the use of a consensus approach in identifying inhibitors of a number of targets, including p38 MAP kinase [18].

A complementary approach to compound acquisition is to prioritize selections based on similarity to known active compounds. A plethora of methods exist for evaluating the similarity of two molecules [41]. Most chemical database systems employ topological similarity metrics based on molecular connectivity. In these methods, chemical structures are represented as sets of constituent functional groups [42,43]. The similarity of pairs of compounds is assessed based on the number of functional groups that the two molecules have in common [44]. The primary advantage of topological methods is their speed. These methods can be used to search millions of molecules in only a few minutes. The disadvantage of these methods is that they tend to be overly literal, identifying only the molecules that are close analogs of the known ligands. The ideal similarity metric will identify molecules that are functionally equivalent to, yet distinct from known ligands. One method of identifying such molecules is to employ a molecular representation based on the three-dimensional structures of the molecules [45]. In this approach, molecules are typically represented as sets of lipophilic, hydrogen bonding and charged groups. Similarity is assessed by comparing the geometric arrangements of these groups. The advantage of these methods is that they tend be more abstract and often lead to identification of new chemical scaffolds. The disadvantage is that the abstract molecular representation is less accurate and can lead to large numbers of false positive results.

The techniques described above provide a means of enriching a screening library with drug-like molecules that contain functionality relevant to targeting the ATP-binding site. Another screening objective is to identify a number of distinct chemical classes. To achieve this goal, we need to ensure that our screening collection is sufficiently diverse. A number of computational approaches to measuring molecular diversity were developed during the 1990s [46]. Most of these techniques operate by calculating a number of molecular descriptors [47]. The descriptor values are then used to define a position in "chemical space" for each molecule [48]. Molecules are then grouped based on their proximity in chemical space. While these techniques have been shown to be applicable in a number of areas [49], it is sometimes difficult to understand the rationale behind the groupings. Simpler techniques, such as the frameworks approach published by Bemis and Murcko [50], create groupings that are much more chemically intuitive. In the frameworks approach, outlined in Fig. (**5**) using a commercial compound as an example, a molecule is successively reduced to an abstract description of a molecular scaffold. These abstract scaffold descriptions can then be used to hierarchically organize molecules. Utilization of

computational tools ensures that whether through acquisition, library synthesis, or structure-based drug design, the compounds that build the kinase collection have an increased probability of producing screening hits that can be rapidly optimized to leads for each kinase.

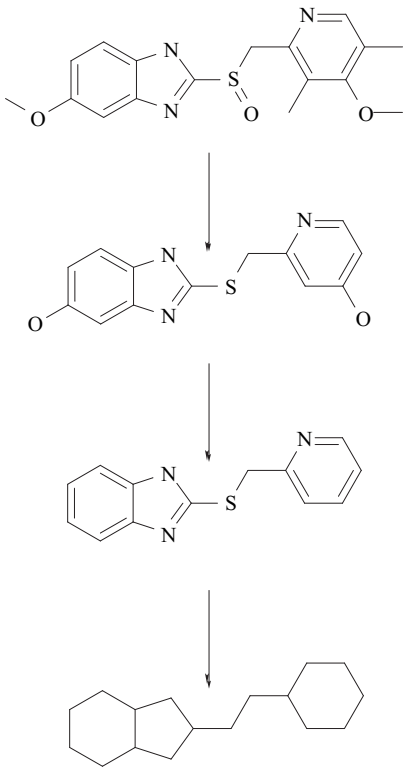

Fig. (5). Frameworks approach to describing a scaffold.

High-Throughput Screening

Populating the screening collection with diverse, drug-like molecules is the first step. The next step is implementing a screening strategy ensuring that hits with a range of binding affinities will be found. One strategy is to screen compounds at lower concentrations (≤ 5 μM) in order to decrease the number of positives and false positives that emerge from the screen [51]. The hypothesis is that screening at higher concentrations (> 10 μM) will identify a greater number of hits but these hits will be of little value as leads, since the activity arises from non-specific interactions with the target. This is clearly a concern, as evidenced by a recent study that has identified aggregation in solution as a common mechanism for non-specific inhibitors [52]. To enable screening at higher compound concentrations, while avoiding a large number of false positives, a high-throughput enzymology (HTE) approach should be implemented. This approach generates quality screening data at higher compound concentrations (e.g. 30 μM) [53], which allows the identification of ligands with a wide range of affinities.

High-throughput enzymology pulls together the automation used for HTS with enzymological assays more traditionally used to support medicinal chemistry. For example, rather than the fixed endpoint assays and IC_{50} values typically generated by HTS, HTE frequently uses kinetic assays and generates K_i values. The automation allows the generation of greater amounts of data and the enzymological assays produce very high quality data. The initial hits are identified from the screen as compounds that show >50% inhibition of the target kinase in the kinetic assay at a fixed concentration. These hits can immediately be titrated to determine K_i values using the same assay. The use of automation greatly facilitates this process. An example of such data is shown in Fig. (**6**) for three screening hits that have been titrated in enzymological screens [53]. Clearly, the titration curves show that the compounds are behaving differently. Compound 1 is the most active compound at 30 μM and would be presumed to be the most potent from the initial HTS data. However, the titration curves show that both compounds 2 and 3 are partial inhibitors of the target kinase. This phenomenon is frequently observed for compounds with poor solubility at higher concentrations. If compounds 2 and 3 are titrated at lower concentrations, they will be found to have significantly lower K_i values than compound 1. More resources are needed since HTE in conjunction with screening at higher concentrations increases

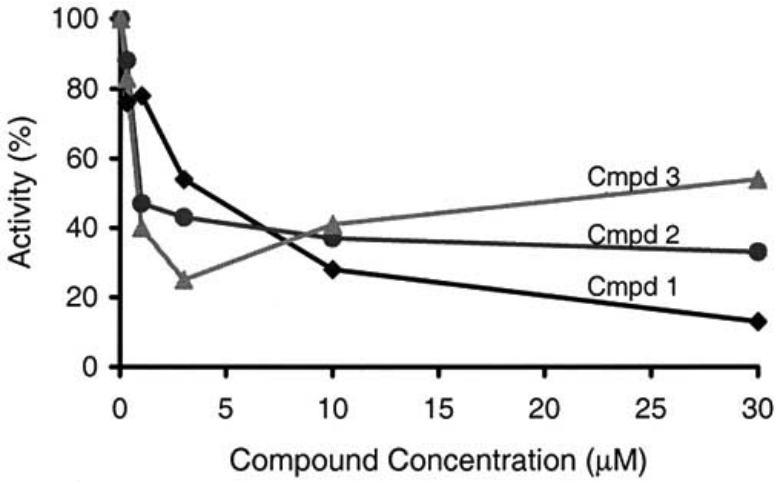

Fig. (6). Examples of dose-response data obtained from counterscreening (reproduced, by permission, from ref. [53]).

Table 1. Standardized Protocol for Confirmation of Hits from High-throughput Screens

Step 1	Medicinal chemists review hits and select candidates for follow-up
Step 2	Purity and identity ➡ Obtain samples of DMSO stock solutions and compound from archive ➡ Evaluate purity by analytical HPLC ➡ Determine molecular weight by mass spectrometry ➡ NMR confirmation of structure
Step 3	Purification of a sample from the archive
Step 4	Enzyme inhibition ➡ Determine Ki ➡ Reversible ➡ Competitive with ATP
Step 5	Evaluate SAR for other analogs in the screen
Step 6	Purchase available analogs from commercial sources
Step 7	Review literature on compound class ➡ Known synthetic routes ➡ Initial assessment of patent literature ➡ Evaluate known physical and biological properties
Step 8	Resynthesize hit and compare to previous results ➡ Purity and identity ➡ Enzyme inhibition
Step 9	Synthesize a set of analogs ➡ Evaluate SAR ➡ Utility of synthetic route for generation of analogs

the number of positives [51]. However, the quality of the data generated by the HTE approach aids in the identification of false negatives due to poor compound solubility and allows better characterization of the compounds in the screening collection.

Hit Confirmation

HTS run at higher concentrations increases the number of hits and their potency range. However, follow-up work is still required to remove false positives and identify the highest quality hits. Starting with a screening collection of quality, drug-like compounds should reduce the numbers of false positives resulting from impurities, reactive functional groups, and poor physical properties. Consequently the effort required to identify false positives is significantly reduced. Unfortunately, no algorithm or selection protocol is 100% effective. For this reason, a standard follow-up strategy (Table 1) is implemented to ensure that hits from every screen are assessed consistently and efficiently.

The first step addresses a deficiency that will exist in any algorithm that is used to assess the drug-likeness of a compound, which is the intuition and knowledge base that an experienced medicinal chemist brings to the process [38]. Years of synthetic and drug discovery experience are brought to bear at the very beginning of the process to choose those hits for follow-up that are most exciting to the medicinal chemists. The remaining steps are designed to reduce the number of hits by determining the answers to some simple questions [27,28]:

- Is the activity reproducible?
- Is the activity an artifact due to an impurity or functionality in the hit?
- Do analogs show dynamic SAR?
- Is the compound tractable to chemical modification?

The purity and identity of the hits are first addressed using standard analytical techniques. Compounds found to be impure must be purified (≥98% by HPLC) and retested. Although in our experience, a majority of the hits identified from screening have been competitive inhibitors at the ATP site, the mechanism of inhibition should be confirmed with this purified sample.

The SAR of the most promising hits must then be evaluated. Initial SAR can be derived from analysis of analogs that are in the screening collection, however, these data should be augmented through the purchase or synthesis of additional analogs. Purchased analogs and small libraries are then assessed in follow-up assays. If a diverse set of analogs around a hit shows only modest changes of activity (< 5 fold), then the SAR around this hit is deemed flat and the hit, along with the scaffold class, becomes a lower priority for lead optimization with this kinase target. These compounds should continue to be screened with each new kinase target since a scaffold that exhibits flat SAR with one kinase, may show potent inhibition and dynamic SAR with a different kinase. For this reason, a validated hit can be either a lead for optimization with a target kinase or a scaffold that can be expanded to provide leads for other kinases. Often, a screening hit is both.

Kinase Leads *vs.* Scaffolds

The difference between a kinase lead and a scaffold is subtle but important. As others have noted, a lead is a starting point for medicinal chemistry optimization [27,28]. Medicinal chemists pursue a specific target kinase and, often a specific indication; therefore, the team works towards a defined compound profile (e.g. potency, selectivity, dosing route, and metabolism). Certainly one of the goals of an optimized lead is to use this compound as a chemogenomic tool to validate the role of a given target kinase in the proposed indication. At this stage, issues surrounding formulation and route of administration are less important; any dosing route (e.g. IV, IP, SC, and PO) that achieves sufficient exposure in the animal model is adequate. The compound should have sufficient selectivity to ensure that pharmacological activity is achieved through inhibition of the target kinase. As the lead compound is optimized, a balance of potency, specificity, and physical properties needs to be achieved. This balance is dependent upon the desired compound profile, which will be dictated by the therapeutic indication and route of administration. For these and other reasons, the chemistry efforts during lead optimization will be highly focused and directed. Pursuing a lead as a kinase inhibitor scaffold, however, will have a different set of goals.

One of the main goals for exploration of a kinase inhibitor scaffold is to build a diverse set of drug-like molecules around the scaffold. This is accomplished by application of computational tools to the virtual library of synthetic targets. Only those compounds that survive the filtering process are then synthesized. The resulting library becomes part of the kinase screening collection and is used in all future kinase screens. In this way, the expanding database contains potency and selectivity data for all compounds with every kinase assayed. With sufficient diverse examples from a scaffold class, a high-throughput enzymology approach to screening yields SAR for both potency and selectivity directly from HTS. Using this information, medicinal chemists can simultaneously evaluate multiple hits from different scaffold classes to determine which scaffold class offers the shortest path to a potent and selective lead. The power of this approach lies in the diversity and drug-like properties of the kinase collection along with the potency and selectivity data that have been generated for each compound.

SELECTIVITY PROFILING AND DATA MANAGEMENT

Inhibitor potency and selectivity data are important for the accurate interpretation of subsequent *in vitro* and *in vivo* assays performed with inhibitors during target validation. A recent publication by Davies clearly illustrates this point [54]. Twenty-eight commercially available compounds, reported to be selective protein kinase inhibitors, were screened against a broad panel of kinases. Several compounds were found to be less selective than previously thought and some inhibited non-target kinases more potently than the kinases for which they were reported to be selective. Another recent report determined that PP1, a reported selective inhibitor of Src family kinases (Src IC_{50} = 170 nM; Lck IC_{50} = 5 nM; Fyn IC_{50} = 6 nM [55]), also inhibits c-Kit ($IC_{50} \approx 75$ nM) [56]. The use of such compounds in the exploration of biochemical pathways and target validation will yield data that may be misinterpreted.

Advances in instrumentation have provided throughput and efficiency such that large sets of compounds can be assayed quickly against a multitude of targets. Even with all the automation at hand, one still cannot realistically assay each compound against every target family member, particularly where the family is as large as the kinases. Therefore, careful consideration must be given to choosing a sufficiently broad "fingerprint" panel of kinases to drive a drug discovery effort.

A gene-family approach can benefit from the use of essentially the same format for all assays in the screening panel. This can result in substantial savings in assay development time, cost, and labor. Spectrophotometric assays are reliable, less prone to interference, and easily implemented [51,57,58]. For kinases it is possible to utilize a spectrophotometric assay, in which the production of ADP by the kinase is coupled to the oxidation of NADH to NAD [59]. This assay format can serve as the basis for most HTE and medicinal chemistry assays. A coupled-enzyme assay can require high concentrations of enzyme to obtain sufficient spectrophotometric readout. Some kinases are difficult to express and purify in large quantities; therefore, assays requiring high enzyme concentrations may not be feasible. For these kinases, there are a number of radiometric and fluorescence-based assays that can be used, which have the advantage of yielding robust signals even at low enzyme concentrations.

Once the profiling assays have been established, it is necessary to consider whether to generate K_i's for compounds with each kinase or to counter screen at one or two inhibitor concentrations *vs*. kinases other than the primary target. K_i values are more reliable and reproducible, since they are determined from multiple data points obtained over a range of inhibitor concentrations. Since a K_i is independent of the substrate concentrations used in the assay, data from two (or more) different sources can be compared. However, for a variety of reasons, one may measure percent inhibition at one or two concentrations. Percent inhibition values can be converted to apparent K_i values assuming competitive inhibition of ATP binding. However, these data should be interpreted conservatively, therefore, it is preferable to assign a K_i range rather than a specific K_i.

For the examples shown in Table 2, each compound was screened at 10 μM and 2 μM against a representative set of fourteen kinases. The percent inhibition data were converted to approximate K_i's and then codified as 2 (K_i <1 μM), 1 (1μM < K_i < 5 μM), and 0 (K_i > 5 μM), which broadly classifies the compounds in terms of the activity against each kinase in the panel. In Table 2, compound V-**07** stands out as a non-selective inhibitor as it scores a 2 for 13 out of 14 kinases. This inhibitor is staurosporine, a known and promiscuous inhibitor of protein kinases. Conversely, examples V-**13** and V-**16** stand out as very selective inhibitors, since they only score a 2 for one kinase and 0 for the other 13 kinases. This summary format is a convenient way to visualize inhibitor selectivity and potency versus a panel of kinases.

Table 2. Selectivity Profile of a Set of Kinase Inhibitors Against Fourteen Kinases

Compd.	AKT3	AR2	CDK2	ERK2	GSK3	JNK3	KDR	lck	MK2	MEK1	p38	src	ZAP70	PKA	Activity Index	Selectivity Index	Inhibitor Score
V-01	0	0	2	0	2	1	0	0	0	0	0	0	0	0	20	79	59
V-02	0	1	0	0	0	1	2	2	0	2	2	2	0	1	52	43	-9
V-03	0	0	0	0	2	2	0	0	0	0	2	0	0	0	21	79	57
V-04	0	2	2	1	2	2	1	0	0	1	1	1	0	0	55	36	-20
V-05	0	2	1	0	2	2	0	1	0	1	0	1	0	1	48	43	-5
V-06	0	2	1	0	2	1	2	2	0	1	0	2	0	0	52	43	-9
V-07	2	2	2	2	2	2	2	2	2	2	0	2	2	2	93	7	-86
V-08	0	1	2	1	2	2	1	1	0	0	0	1	1	1	59	29	-30
V-09	0	2	2	1	2	2	2	2	1	2	0	2	0	1	73	21	-52
V-10	0	0	0	1	1	0	0	0	0	0	0	0	0	1	16	79	63
V-11	0	2	1	0	0	0	2	2	0	2	0	2	0	0	41	57	16
V-12	1	2	1	2	2	1	1	2	1	0	0	2	0	2	70	21	-48
V-13	0	0	0	0	0	0	0	0	0	2	0	0	0	0	7	93	86
V-14	0	2	2	0	2	0	2	2	0	1	0	2	0	1	54	43	-11
V-15	0	1	0	0	2	0	0	1	0	0	0	2	0	0	25	71	46
V-16	0	0	0	0	0	2	0	0	0	0	0	0	0	0	7	93	86
V-17	0	2	2	0	2	1	2	1	0	0	0	2	0	0	46	50	4
V-18	0	0	1	1	2	2	0	0	0	0	2	0	0	0	32	64	32
V-19	2	1	1	1	1	0	0	0	1	0	0	0	0	0	34	57	23

Inhibitor codes calculated for each compound as outlined in the text

The coded data in Table 2 can be further reduced into one or two parameters that describe the characteristics of each inhibitor more comprehensively. Since any reasonable definition of the "activity" of an inhibitor requires consideration of both its overall potency and its range of activity, the characteristics of each inhibitor can be defined in terms of two parameters, the inhibitor activity index, A_I (Eqn. **1**) and the selectivity index, S_I (Eqn. **2**). The inhibitor activity index can be regarded as a composite value, which takes into account the number of kinases, N_I, in a given panel inhibited by the compound (score of 1 or 2), the total number of kinases in the panel, N_T, and the sum of the scores for that compound in the panel, C_{sum}.

Eqn. **1** $A_I = [(2N_I + C_{sum})/4N_T] \times 100$

Eqn. **2** $S_I = \{1 - [N_I/(N_T - 1)]\} \times 100$

Eqn. **3** $I^* = S_I - A_I$

The value of A_I varies between 0 and 100 and the magnitude of A_I correlates directly with broader activity towards the kinases in a panel. A lower activity index implies more restricted activity. The inhibitor selectivity, S_I, also ranges between 0 and 100. The higher the S_I value of a compound, the greater is its selectivity. Inhibitor activity and selectivity contribute in opposite ways in defining the overall potency of an inhibitor as it undergoes medicinal chemistry optimization; therefore, an additional parameter called inhibitor score, I^* (Eqn. **3**) is used. The value of I^* can fall between –100 and 100. A compound with a large, negative inhibitor score will be a non-specific inhibitor, while the compound with a large, positive value would be highly selective. As shown in Table 2, the selectivity data for compounds have been processed to yield the parameters. The inhibitor scores in Table 2 are plotted in Fig. (**7**). The designation of "regions of selectivity and non-selectivity" is arbitrary; however, these empirical formulations provide a method of gauging and comparing the *in vitro* potency and selectivity of inhibitors. These simple visualization tools aid the medicinal chemist in evaluating progress during lead optimization (e.g. A_I decreases, S_I increases, and I* is maximized) or in comparing hits from HTS.

Inhibitor-based ATP Site Homology

Affinity data for a diverse collection of inhibitors can be used to analyze the ATP sites of different targets. The traditional way to estimate this relatedness is through amino acid homology and has been performed for the human kinome[4]; however, this measure can be further refined for the purpose of drug design by using the inhibitor affinity data. Earlier work has suggested that affinity fingerprinting with small molecules could be used to measure similarity between proteins [60]. Subsequently, Frye proposed that groups of kinases that are inhibited by ATP competitive inhibitors may be very different from groupings based on amino acid homology or biochemical function [61]. This approach is termed structure-activity relationship homology (SARAH) and uses small molecules to sort members of a gene family. We have performed a similar analysis for the ATP site of kinases based on several years of kinase library synthesis and inhibitor screening.

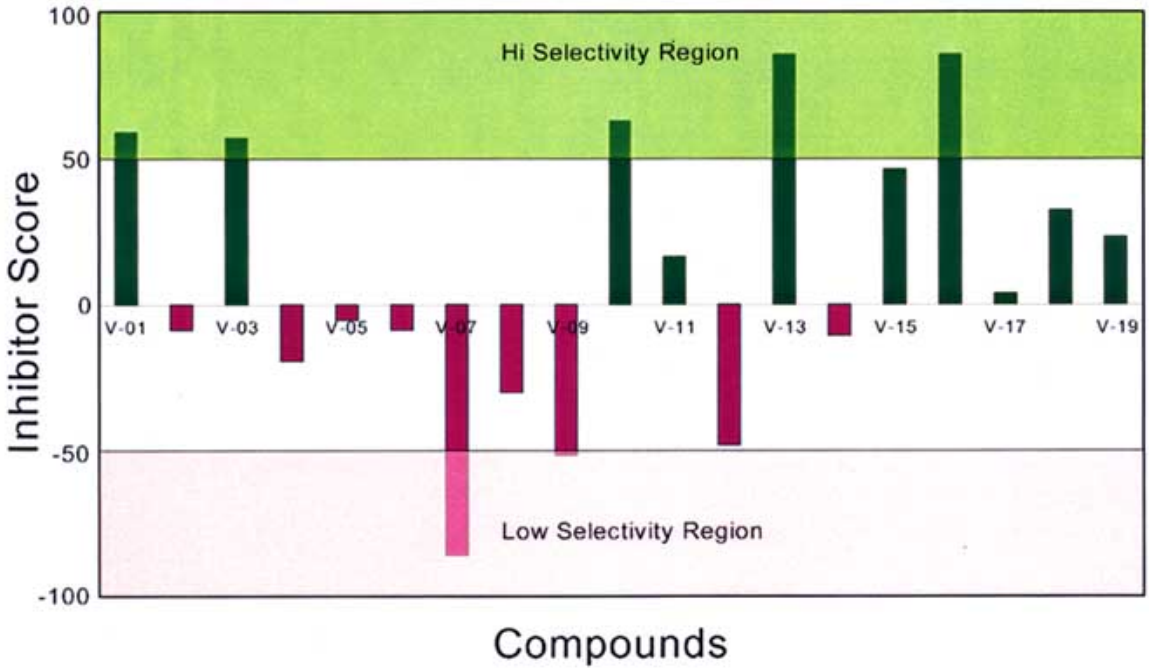

Fig. (7). A graphical representation of the inhibitor scores from Table 2.

For this analysis, only K_i values determined by titrations were used. Compounds were excluded if inhibition data on fewer than three kinases were available and kinases were excluded if fewer than 150 active (K_i <2.5 μM) inhibitors were available. With the resulting set of 4029 kinase inhibitors and thirteen kinases, a matrix of codes (0, 1 and 2 for >2.5 μM, 0.25 – 2.5 μM, and <0.25 μM, respectively) was generated. The definition of these codes differs from the codes above due to the larger number of titrations carried out at lower inhibitor concentrations in these K_i determinations. These codes were then used to analyze the similarity between kinases (details of this analysis will be published elsewhere). The results of this analysis suggest that kinase families based on SAR homology will in fact be very different from those based on sequence similarity or shared biochemical function. Fig. (**8a**) shows the clustering of the 13 kinases from the data set based on sequence similarity and Fig. (**8b**) shows the same clustering based on SAR similarity. While

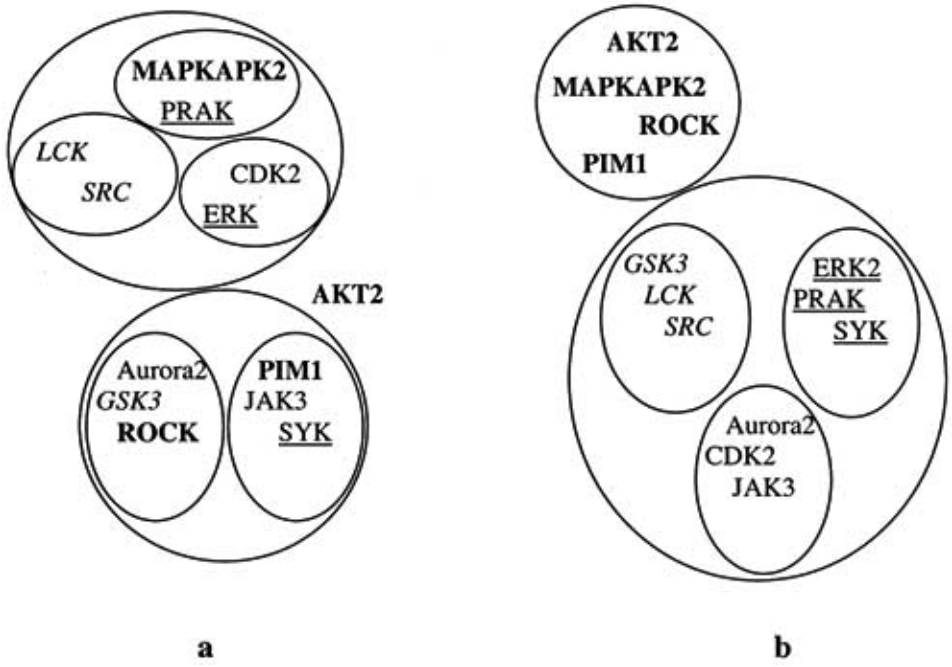

Fig. (8). (**a**) Thirteen kinases were clustered according to their sequence homology. This can be compared to (**b**) the same kinases clustered according to their SAR homology.

there are some similarities -- the closely related kinases Src and Lck cluster with both methods -- for the most part the two clusters are very different.

While it seems surprising at first to find such poor correlation between sequence similarity and kinase inhibition similarity, there are some fundamental reasons why this might be expected. First, there are the general limitations of sequence similarity analysis to be considered. Sequence analysis does not take into account whether the side-chain of a residue points into the active site or how flexible the active site is within a given stretch of sequence. Both of these factors will strongly influence ligand binding and have a large effect on binding site similarity that is not reflected in sequence similarity. There are at least two extreme cases reported where a single amino acid mutation radically alters the specificity profile of a given kinase inhibitor. In the first case, the mutation of residue 105 in ERK2 leads to a greater than 25,000-fold sensitization of this enzyme to the selective p38 inhibitor, SB202190 [18,62]. More recently, it has been shown that mutation of the corresponding residue in the Flt-3 and PDGFβ receptor tyrosine kinases can completely invert the selectivity of STI-571 towards these two kinases [63]. Given the extreme sensitivity of kinase inhibition to the mutation of a single active site residue, it should not be surprising that the overall active site sequence similarity serves as a poor predictor of inhibition similarity.

Target Hopping

One of the underlying assumptions of chemogenomics is that inhibitor analogs will bind to similar targets within a gene family. Inhibitor profiling versus a kinase panel has shown this assumption to be true for the kinase gene family. The similarity of the ATP site was originally used to argue that kinases were poor targets because they bind ATP in a similar configuration and might bind inhibitors with equal affinity, making selectivity difficult to achieve. However we now know that kinases possess a rich variety of shape variations contiguous with the ATP-binding site that enables the design of selective inhibitors. We also know that the degree of similarity between ATP-binding sites can be used to our advantage in identifying scaffolds with binding motifs recognized by many kinase targets. The combination of the similarity of kinase ATP-binding sites with the structural differences in close proximity makes it likely that once an inhibitor is found for a single kinase, it will be possible to find analogs of that ligand which inhibit other kinases. We refer to this as "Target Hopping," which allows the use of a kinase inhibitor scaffold across multiple targets within the family.

As an example of compounds from the same scaffold hitting different kinases, consider the 3-Methylene-1,3-dihydro-indol-2-one scaffold shown in Fig. (**9**). A substructure search of the iddb3 database (www.iddb3.com) finds at least 60 different patents from more than 10 different organizations. These patents are directed against at least 14 different kinase targets (including c-kit, CDK1-9, c-Src, EGF, FGFR1, Flk-GST, GSK-3β, FRK, IGF, JNK, PDGF, Raf, TrkA, VEGF) and 2 non-kinase targets (GAR transformylase and the 5-HT receptor). A similar analysis could easily be performed for several other prominent kinase inhibitor scaffolds. Once a compound in a chemical class is discovered to be an inhibitor for a target in a gene family, screening compounds in the same inhibitor class against targets within the same gene family has increased odds of success.

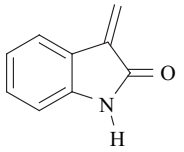

Fig. (9). 3-Methylene-1,3-dihydro-indol-2-one.

Scaffold Morphing

Chemogenomics enables the use of a combination of inhibitor profiling and x-ray crystallographic data to predict the structure modifications of an inhibitor of one kinase that will enable binding to the active site of a different kinase. This gives rise to a drug design process that can generate new scaffold variations not envisioned by considering only a single target. The ability to use kinase structural information to design new scaffolds as kinase inhibitors is referred to as "scaffold morphing." This process relies on an understanding of several factors: (1) how the three-dimensional structures of different kinases overlap; (2) the three-dimensional structure for an inhibitor bound to a kinase; (3) an understanding of the theoretical binding orientation of an inhibitor to a different kinase; and (4) the ability to understand how structural changes or "morphing" of the inhibitor would be expected to improve the binding affinity to the new kinase. The final section of this review will present specific examples of "hopping" a scaffold from one kinase to another and also examples of using structural insights for "morphing" a scaffold into a new inhibitor class.

CHEMOGENOMIC EXAMPLE: DESIGN OF INHIBITORS FOR THE SAPKs

This section highlights the discovery efforts leading to a potent, selective p38 mitogen activated protein (MAP) kinase inhibitor, VX-745 (Fig. (**4**)). Structural studies focused on producing a detailed understanding of the bound crystal structure of VX-745 in complex with p38. The molecular basis for understanding both the potency and selectivity of the compound coupled to the utilization of the chemogenomic approach and tools described above, served as a platform that provided both alternate scaffolds for p38 as well as new classes of inhibitors for other kinases.

Inhibitors of p38 block the production of the pro-inflammatory cytokines TNF-α and IL-1β and are effective in animal models of sepsis and arthritis [64]. TNF-α and IL-1β are inducible, pleiotropic cytokines and are central regulators of immune and inflammatory responses [65]. Over-expression of TNF-α and IL-1β is associated with human diseases [66,67] such as rheumatoid arthritis, Crohn's disease, psoriasis, fever, lethal shock, tissue injury, and weight loss. Protein therapeutics, such as Etanercept (a soluble TNF-α receptor) [68,69], and Infliximab (a monoclonal antibody to TNF-α) [70-72] have been used clinically for the treatment of rheumatoid arthritis and Crohn's disease. Furthermore, dual inhibition of both TNF-α and IL-1β using protein antagonists produced synergistic

effects in animal models of arthritis and osteoporosis, indicating potential clinical and commercial benefits in simultaneously blocking both cytokines [99].

Pyridinylimidazole compounds, exemplified by SB 203580 and VK-19911 in Fig. (**4**), block the production of IL-1β and TNF-α from monocytes stimulated by LPS through the inhibition of p38 [18,73]. These compounds have been used as tools to investigate the role of p38 MAP kinase in intracellular signal transduction pathways and have provided a structural understanding of p38 inhibition. Both compounds are selective for p38α and p38β, and do not inhibit p38γ, p38δ, or other MAP kinase family members, such as the extracellular-signal regulated kinases (ERKs) or most isoforms of the c-Jun N-terminal kinases (JNKs) [74-76].

The crystal structure of unphosphorylated p38 MAP kinase bound to VK-19911 has been reported [18]. Analysis of this co-complex proved to be a powerful tool for the discovery of novel inhibitors of p38. Utilizing lead molecules from the literature, including ATP analogs and pyrimidinyl imidazoles, virtual screening of the available chemical databases provided a directed library of compounds as potential p38 ATP site inhibitors (Bemis, G. W., Vertex Pharmaceuticals, Inc., personal communication). The compounds selected by this process had similar shape yet differing chemical connectivity when compared to the virtual leads. Using this method, we identified several low micromolar leads and focused on a novel bicyclic pyridazine scaffold that ultimately yielded VX-745 [77].

Table 3. VX-745 Selectively Inhibits p38α MAP Kinase

Kinase	IC_{50} (μM)
p38- α	0.009
p38-β	0.22
p38-γ	>100
p38-δ	>100
ERK2	>100
JNK3	>100
lck	>20
p60c-src	>20
fyn	>20
MAPKAP K-2	>20

VX-745 is a potent and specific inhibitor of p38α with an IC_{50} of 9 nM (Table 3). The compound is 24-fold less potent against p38β and displays no appreciable inhibition of p38γ or p38δ, even at a concentration of 100 μM. To understand the molecular basis for the potency and selectivity of VX-745, the X-ray crystal structure of unphosphorylated p38 MAP kinase bound to VX-745 was solved and is shown in Fig. (**10**). VX-745 forms hydrogen bonds with the backbone amide nitrogen atoms of two hinge residues, Met109 and Gly110. A more detailed structure in Fig. (**11**) shows that, relative to the conformation in the unliganded structure, a 180° rotation of the Gly110 carbonyl group occurs to allow the hydrogen bond between the inhibitor and Gly110. The rotation removes an unfavorable contact and permits the backbone amide nitrogen of Gly110

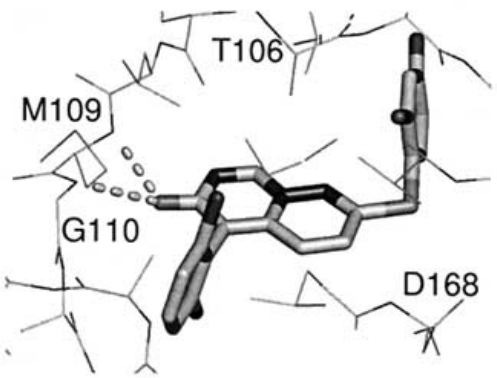

Fig. (10). Active site of p38 in complex with VX-745.

to donate a proton to the inhibitor carbonyl at C-6. The 2,4-difluorophenyl ring of VX-745 occupies a hydrophobic pocket and makes van der Waals contacts with multiple residues. These contacts are essentially identical to the van der Waals interactions between the para-fluoro phenyl ring of VK-19911 and p38 [18]. As observed for VK-19911, Thr106 in Fig. (**10**) rotates 120° about χ-1. This rotation alters the position of the γ-hydroxyl moiety and generates additional hydrophobic contacts with the fluorophenyl ring. The interaction between the 2,6-dichlorophenyl ring of VX-745 and p38 is stabilized by van der Waals interactions. Each chlorine atom occupies a hydrophobic pocket and the phenyl ring makes favorable van der Waals interactions with residues Gly110, Ala111 and Asp112. The para position of this ring faces bulk solvent.

Based upon the structural features described above for VX-745 and VK-19911, it is clear that the rotation about the side chain of Thr106 plays a key role in determining the selectivity of these compounds for p38. In fact, the larger side-chains at position 106 in p38γ (Met) and ERK2 (Gln) render these MAP kinases resistant to inhibition by VX-745. Thus the residue corresponding to Thr106 in other MAP kinases may be a critical determinant of specificity for VX-

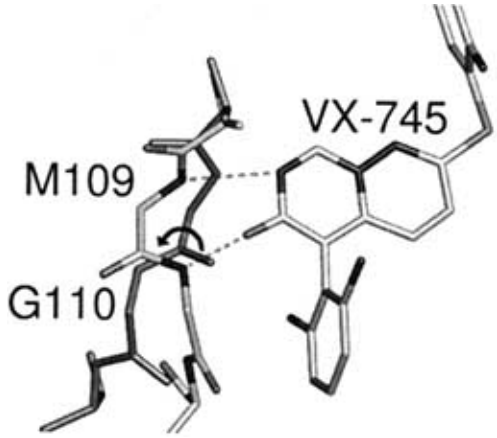

Fig. (11). The structure of the apo, unphosphorylated form of p38 is compared with the refined structure of the VX-745 complex. Backbone rotation circumvents a potential clash between Met 109 carbonyl and the inhibitor carbonyl and allows the backbone amide nitrogen of Gly110 to donate a proton to the inhibitor carbonyl.

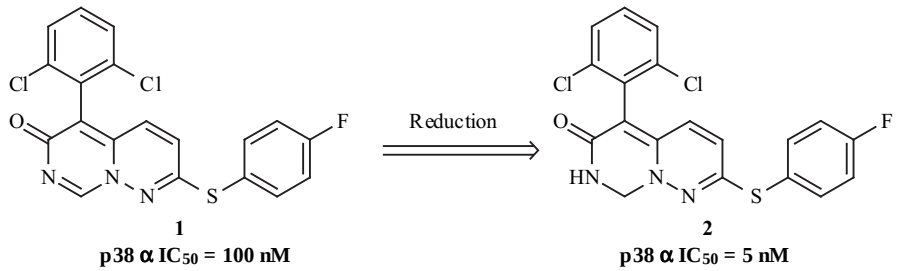

Fig. (12). Compounds of the VX-745 class can easily be reduced to the 7,8 dihydro-scaffold represented by **2**.

745. The 2,6-dichlorophenyl ring makes contacts with Gly110, Ala111, and Asp112, residues that are not

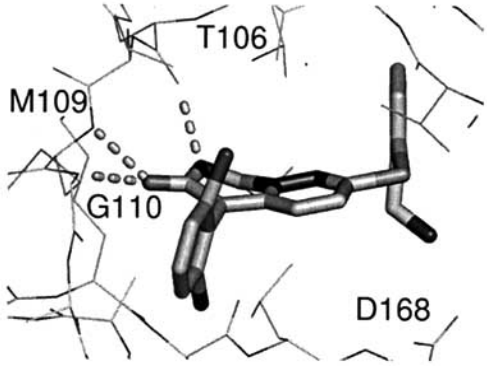

Fig. (13). Crystal structure of an analog of **2** bound to p38.

conserved in other kinases, further enhancing the selectivity of VX-745. The 180° backbone rotation, shown in Fig. (**11**), establishes a favorable hydrogen bond between the inhibitor carbonyl and the NH of Gly110. The presence of a Gly at position 110 may permit the backbone rotation, since the ϕ and ψ angles for Gly110 in the p38/VX-745 complex translate to disallowed regions of the Ramachandran plot if other amino acids are present in this position (i.e. only Glycine can exist in a low energy conformation with the angles observed in the complex). A perusal of one database of aligned kinase sequences shows that less than 10 out of 390 kinases have a Glycine residue in this position [78]. This allows us to speculate that VX-745 and other inhibitors that utilize this binding motif will achieve good selectivity against kinases with bulky amino acid side-chains at position 110. Consistent with the importance of the Gly110 ϕ/ψ conformation, a Gly110Asp mutation in p38 significantly reduces binding of VX-745 to the mutant enzyme (Salituro, F. G., Vertex Pharmaceuticals, Inc., personal communication).

While favorable binding interactions are observed in the crystal structure of VX-745 and p38, one potentially unfavorable interaction led to a proposed set of new inhibitors. The crystal structure revealed a close contact between the N-7 of VX-745 and the carbonyl of residue 108

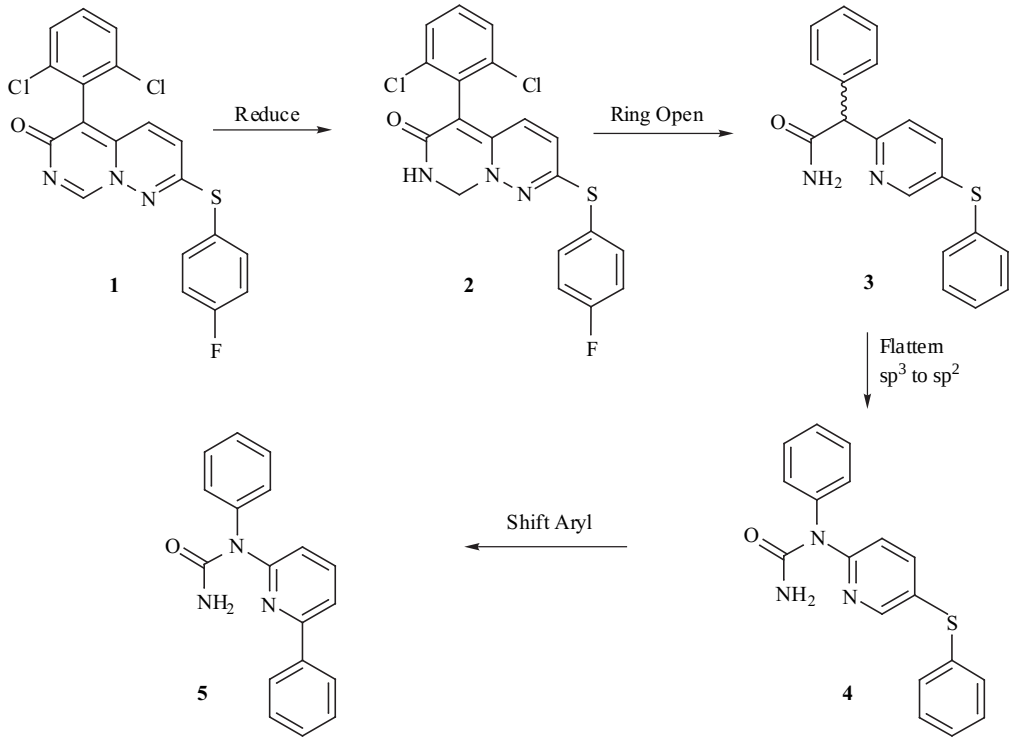

Fig. (14). Evolution of VX-745 scaffold to second generation scaffolds.

that could translate into a detrimental interaction. Models suggested that a "reduced" scaffold [Fig. (**12**), compound **2**] would provide an additional favorable hydrogen bond. This analog was prepared and found to be approximately 20-fold more potent than the parent. The crystal structure of another such compound in Fig. (**13**) shows essentially an identical binding mode relative to the oxidized parent but with additional hydrogen bond contacts as highlighted.

PK liabilities of the "reduced" scaffold precluded pursuit of this series; however, the structural understanding led to the design of new scaffolds as illustrated in Fig. (**14**). We envisioned that scaffold morphing to the ring-opened compounds (compounds **3**-**5**) could retain both the 3-dimensional features and the hydrogen bonding capabilities of the "reduced scaffold" (compound **2**). Ring-opened compounds of this type could be held in a favorable conformation via an intra-molecular hydrogen bond between

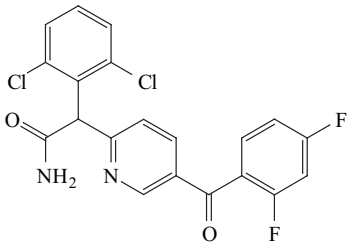

6

JNK3 K_i = 700 nM
p38α K_i = 400 nM

Fig. (15). Chemical structure of **6**, an equipotent inhibitor of p38 and JNK3.

the pyridine nitrogen and the primary amide (or urea) and retain full hydrogen bonding capability to the enzyme with the second NH of the amide or urea moiety. The necessity for a chiral sp^3 carbon in place of the C-5 sp^2 carbon bearing the 2,6-dichlorophenyl ring in VX-745, is one major change between compound **3** and the previous scaffolds. However, further modification to the N, N-disubstituted urea (compounds **4** and **5**) would flatten the molecule and provide even closer mimics of VX-745. Modeling also suggested that the hydrophobic pocket could be accessed by either an "S-phenyl" substituent at the 5 position of the pyridine (compound **4**) or direct phenyl attachment at the 6 position as shown for compound **5**. Medicinal chemistry exploration in each of the series outlined in Fig. (**14**) resulted in potent, selective compounds for p38 in addition to a wealth of structural information and SAR [79].

While the majority of compounds in these series were selective for p38α, some compounds showed cross-inhibition with other MAP kinases, specifically JNK3. Compound **6** in Fig. (**15**) was essentially equipotent for p38α and JNK3 (400 nM and 700 nM, respectively), and the X-ray crystal structures of **6** bound to both kinases were solved. The structure of the compound bound to p38α in Fig. (**16a**) revealed few surprises relative to other amide and urea inhibitors in p38α. Similar to related compounds, binding of this inhibitor class induced a backbone rotation about Gly110 to accommodate hydrogen bonding between inhibitor and enzyme. The bound structure of compound **6** in JNK3 in Fig. (**16b**) was interesting in that, as postulated from the p38 structures, there was no backbone rotation about the hinge region at residue Asp150, the equivalent of Gly110 in p38. Instead, there appeared to be a rotation of the primary amide of the molecule itself such that favorable hydrogen bonding interactions with the hinge could be established without enzyme backbone rotation. This proposal is based on inference, since the X-ray structure cannot unambiguously distinguish between the nitrogen and the oxygen of the primary amide moiety; the distance (2.9-3.4 Å) and the pairing of hydrogen bond donors/acceptors versus potential clashes between ligand and enzyme suggests the amide rotation. In addition, the surprising result that unambiguously places the fluorophenyl ketone of this inhibitor in the hydrophobic pocket was striking in that it was previously thought that this pocket in JNK3 could not

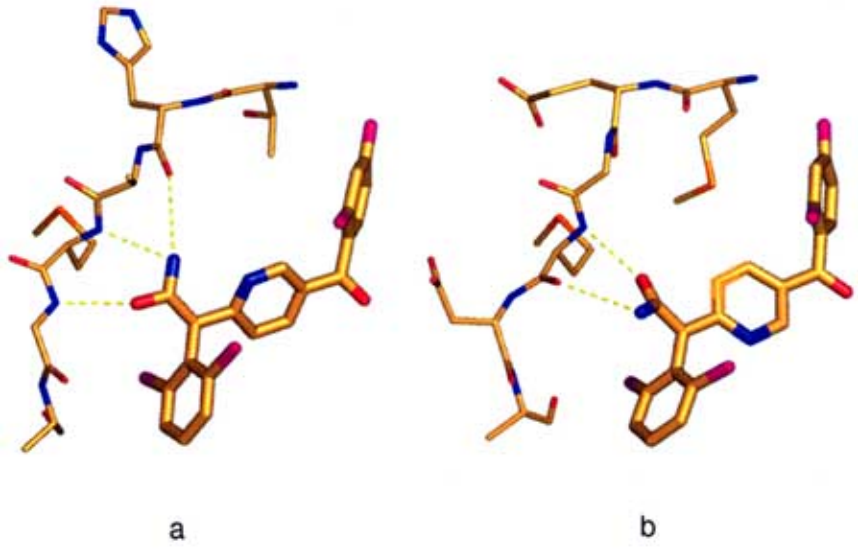

Fig. (16). Crystal structure of **6** in (**a**) p38 vs. (**b**) JNK3.

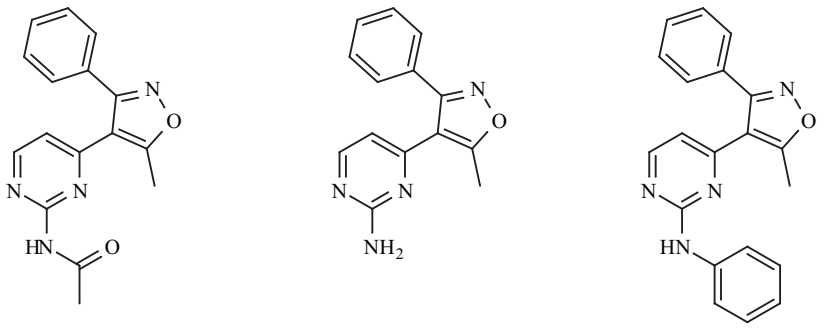

7

JNK3 K = 0.79 uM
p38a 70% @ 2uM

8

JNK3 K_i = 2.3 uM
p38a K_i = 3.2 uM

9

JNK3 K_i = 0.025 uM
p38a K_i = 0.056 uM

Fig. (17). Structures of isoxazole-based dual p38/JNK3 inhibitor leads.

be accessed due to the steric bulk of the Met146 residue. Although the scaffold did not formally become a JNK inhibitor class ("target hop"), it did serve as the starting point for a strategy to develop dual p38/JNK3 inhibitors. Dual inhibition as it related to potential therapies for stroke, addressing both anti-apoptotic component (JNK3) and inflammatory component (p38) of the disease, was of keen interest [80-82].

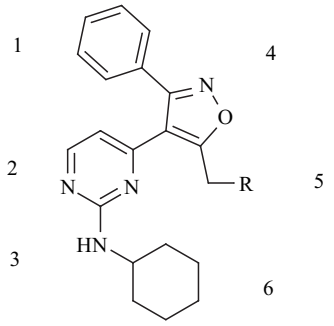

Fig. (18). SAR exploration for isoxazole-based dual p38/JNK3 inhibitors.

Further directed screening using the established binding motifs (backbone hydrogen bonding and hydrophobic pocket binding) resulted in several screening hits in Fig. (**17**) that were pursued by medicinal chemistry efforts, one of which led to the identification of compound **7** [83,84]. Early SAR indicated that, while less active, compound **8** still retained significant potency against JNK3. Further exploration of possible N-substituents subsequently identified compound **9** as a viable lead for further optimization.

Extensive SAR studies of the general structure in Fig. (**18**) were guided by SBDD, which was driven by numerous X-ray crystal structures of enzyme-inhibitor co-complexes. The medicinal chemistry efforts focused on 6 specific regions of the molecule, with regions 1, 5 and 6 proving to be of particular importance for varying the selectivity profiles of the compounds. Compounds with bulky aromatic substituents in region 1 displayed dual p38/JNK3 activity. The binding mode for compounds in this class is nearly identical for both enzymes including, as predicted, the region of the hydrophobic pocket gated by Thr106 and Met146 in p38 and JNK3, respectively. It is assumed that the energy cost of the movement of Met146 in JNK3 is sufficiently compensated by the positive binding interaction of the phenyl group. In addition, compounds with aromatic substituents in both regions 1 and 6 (e.g. compound **10** in Fig. (**19**)) also display strong inhibitory potency against Src-family kinases. However, replacement of the N-aryl group in region 6 with a saturated ring, as exemplified by compounds **11** and **12** in Fig. (**19**), eliminated inhibition of the Src-family kinases, while maintaining JNK3 and p38 activity.

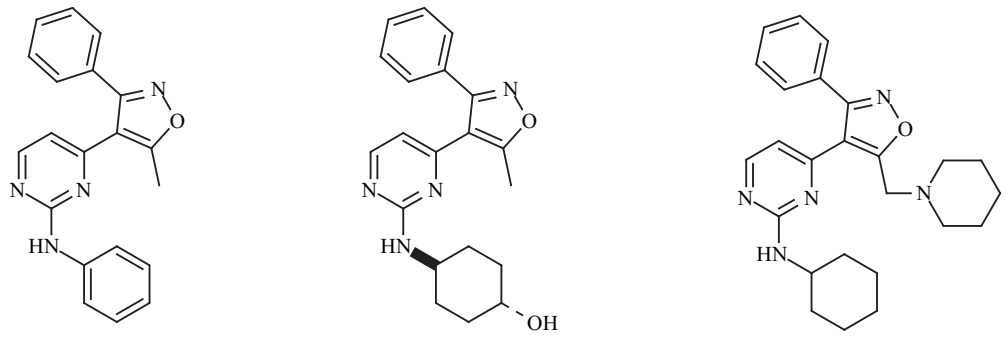

10

JNK3 K_i = 0.025 μM
p38α K_i = 0.056 μM
Src K_i = 0.60 μM

11

JNK3 K_i = 0.002 μM
p38α K_i = 0.008 μM
Src K_i = 18 μM

12

JNK3 K_i = 0.002 μM
p38α K_i = 0.026 μM
Src 6% inhibition & 2 μM

Fig. (19). Potent dual inhibitors of p38/JNK3.

The inhibition of Src by compound **10** indicated a potential "target hop" for this scaffold. These observations were a starting point for developing a strategy towards the selective inhibition of Src-family kinases for which there is significant interest in regards to a variety of therapeutic indications, such as immunosuppression [85,86]. Indeed, utilizing the isoxazole starting point and the chemogenomic strategies discussed, novel classes of potent Src-family inhibitors have been discovered that select away from inhibition of other SAPK family members [87].

X-ray crystallography and modeling further suggested that substitution in region 5 would be an ideal strategy for addressing the physical properties of the inhibitors without adversely affecting the enzyme activity. Thus, a series of compounds (e.g. compound **12** in Fig. (**19**)) containing amine moieties in region 5 were prepared and found to be more soluble while retaining potent dual JNK3/p38 activity. These compounds exhibited high aqueous solubility as the hydrochloride salts and were suitable for dosing in aqueous vehicles.

Overall, this section has shown the successful application of the chemogenomic principles that were outlined in the first part of this review. Computational tools and X-ray crystallographic structures enabled the identification of inhibitors of p38α, which produced the selective inhibitor VX-745. Structure-based understanding of this compound's binding to the ATP site of p38 allowed morphing of this scaffold into new p38 inhibitor scaffolds. Because of the gene family approach to kinases, we found that these new kinase scaffolds enabled a target hop to another kinase, JNK3. In a parallel fashion, computational tools applied to directed screening provided additional chemical leads for JNK3, which were used by medicinal chemists to drive structure-based drug design, resulting in novel inhibitor scaffolds. Again, the gene family approach identified leads from these scaffolds that inhibited c-Src, which enabled a target hop to the Src-family of kinases.

Because of the broad, chemogenomic approach to kinase inhibitor scaffolds, leads identified for just these three targets, p38, JNK3, and c-Src, resulted in the addition of well over 2 dozen distinct inhibitor scaffolds to the inhibitor collection. As these scaffolds expanded the diversity of the compound collection, counter-screening expanded the knowledge base on kinase inhibition and selectivity. Much of this expansion of knowledge was done in parallel utilizing HTE with multiple kinases. The knowledge base of inhibitor potency and selectivity was complemented with structural information from crystallography in as close to real time as possible. It is readily apparent from the small number of examples reviewed here that the data for each kinase target and scaffold class quickly grows and serves to drive the expansion into new kinase targets. A chemogenomic approach increases the odds of rapidly identifying leads from HTS for each kinase target. The wealth of existing structural and SAR data available for the leads then facilitates the optimization process to provide the compounds for validation of those kinases. Following validation of the kinase as a potential therapeutic target, these optimized leads are poised for rapid refinement to provide a compound that is a strong candidate for preclinical evaluation.

LIST OF ABBREVIATIONS

Abl	=	Abelson leukemia virus tyrosine kinase
AKT	=	Protein kinase B
AMPPNP	=	Adenosine 5'-(β,γ-imido)triphosphate
AR2	=	Aurora 2 kinase
Btk	=	Brutons tyrosine kinase
CDK	=	Cyclin dependent kinase
CSK	=	c-Src kinase
DELFIA	=	Dissociation enhanced fluorescent immunoassay
EGFR	=	Epidermal growth factor receptor
Ephb2R	=	Ephrin b2 receptor
ERK	=	Extracellular signal-regulated kinase
FGFR	=	Fibroblast growth factor receptor
FRK	=	Fyn-related kinase
GSK-3β	=	Glycogen synthase kinase-3β
Hck	=	Haematopoietic cell kinase
5-HT	=	5-Hydroxytryptamine
HTRF	=	Homogenous time resolved fluorescence
IGFR	=	Insulin-like growth factor receptor
IL-1β	=	Interleukin-1β
INSR	=	Insulin receptor kinase
KDR	=	Kinase insert domain receptor/VEGFR2
Kit	=	Stem cell factor receptor
MK2 or MAPKAP-K2	=	MAPK-activated protein kinase-2
MAPK	=	Mitogen-activated protein kinase
MEK1	=	MAPK kinase
PDGFR	=	Platelet-derived growth factor receptor
PKA	=	Protein kinase A
SAR	=	Structure-activity relationships
TNF-α	=	Tumor necrosis factor-α
VEGFR	=	Vascular endothelial growth factor receptor

REFERENCES

[1] Venter, J. C.; Adams, M. D.; Myers, E. W.; Li, P. W.; Mural, R. J.; Sutton, G. G.; Smith, H. O.; Yandell, M.; Evans, C. A.; Holt, R. A.; Gocayne, J. D.; Amanatides, P.; Ballew, R. M.; Huson, D. H.; Wortman, J. R.; Zhang, Q.; Kodira, C. D.; Zheng, X. H.; Chen, L.; Skupski, M.; Subramanian, G.; Thomas, P. D.; Zhang, J.; Gabor Miklos, G. L.; Nelson, C.; Broder, S.; Clark, A. G.; Nadeau, J.; McKusick, V. A.; Zinder, N.; Levine, A. J.; Roberts, R. J.; Simon, M.; Slayman, C.; Hunkapiller, M.; Bolanos, R.; Delcher, A.; Dew, I.; Fasulo, D.; Flanigan, M.; Florea, L.; Halpern, A.; Hannenhalli, S.; Kravitz, S.; Levy, S.; Mobarry, C.; Reinert, K.; Remington, K.; Abu-Threideh, J.; Beasley, E.; Biddick, K.; Bonazzi, V.; Brandon, R.; Cargill, M.; Chandramouliswaran, I.; Charlab, R.; Chaturvedi, K.; Deng, Z.; Di Francesco, V.; Dunn, P.; Eilbeck, K.; Evangelista, C.; Gabrielian, A. E.; Gan, W.; Ge, W.; Gong, F.; Gu, Z.; Guan, P.;

Heiman, T. J.; Higgins, M. E.; Ji, R. R.; Ke, Z.; Ketchum, K. A.; Lai, Z.; Lei, Y.; Li, Z.; Li, J.; Liang, Y.; Lin, X.; Lu, F.; Merkulov, G. V.; Milshina, N.; Moore, H. M.; Naik, A. K.; Narayan, V. A.; Neelam, B.; Nusskern, D.; Rusch, D. B.; Salzberg, S.; Shao, W.; Shue, B.; Sun, J.; Wang, Z.; Wang, A.; Wang, X.; Wang, J.; Wei, M.; Wides, R.; Xiao, C.; Yan, C. *Science* **2001**, *291*, 1304.

[2] Lander, E. S.; Linton, L. M.; Birren, B.; Nusbaum, C.; Zody, M. C.; Baldwin, J.; Devon, K.; Dewar, K.; Doyle, M.; FitzHugh, W.; Funke, R.; Gage, D.; Harris, K.; Heaford, A.; Howland, J.; Kann, L.; Lehoczky, J.; LeVine, R.; McEwan, P.; McKernan, K.; Meldrim, J.; Mesirov, J. P.; Miranda, C.; Morris, W.; Naylor, J.; Raymond, C.; Rosetti, M.; Santos, R.; Sheridan, A.; Sougnez, C.; Stange-Thomann, N.; Stojanovic, N.; Subramanian, A.; Wyman, D.; Rogers, J.; Sulston, J.; Ainscough, R.; Beck, S.; Bentley, D.; Burton, J.; Clee, C.; Carter, N.; Coulson, A.; Deadman, R.; Deloukas, P.; Dunham, A.; Dunham, I.; Durbin, R.; French, L.; Grafham, D.; Gregory, S.; Hubbard, T.; Humphray, S.; Hunt, A.; Jones, M.; Lloyd, C.; McMurray, A.; Matthews, L.; Mercer, S.; Milne, S.; Mullikin, J. C.; Mungall, A.; Plumb, R.; Ross, M.; Shownkeen, R.; Sims, S.; Waterston, R. H.; Wilson, R. K.; Hillier, L. W.; McPherson, J. D.; Marra, M. A.; Mardis, E. R.; Fulton, L. A.; Chinwalla, A. T.; Pepin, K. H.; Gish, W. R.; Chissoe, S. L.; Wendl, M. C.; Delehaunty, K. D.; Miner, T. L.; Delehaunty, A.; Kramer, J. B.; Cook, L. L.; Fulton, R. S.; Johnson, D. L.; Minx, P. J.; Clifton, S. W.; Hawkins, T.; Branscomb, E.; Predki, P.; Richardson, P.; Wenning, S.; Slezak, T.; Doggett, N.; Cheng, J. F.; Olsen, A.; Lucas, S.; Elkin, C.; Uberbacher, E.; Frazier, M. *Nature* **2001**, *409*, 860.

[3] Hopkins, A. L.; Groom, C. R. *Nature Rev. Drug Disc.* **2002**, *1*, 727.

[4] Manning, G.; Whyte, D. B.; Martinez, R.; Hunter, T.; Sudarsanam, S. *Science* **2002**, *298*, 1912.

[5] Caron, P. R.; Mullican, M. D.; Mashal, R. D.; Wilson, K. P.; Su, M. S.; Murcko, M. A. *Current Opinion in Chemical Biology* **2001**, *5*, 464.

[6] Knuutila, S.; Bjorkqvist, A.-M.; Autio, K.; Tarkkaqnen, M.; Wolf, M.; Monni, O.; Szymanska, J.; Larramendy, M. L.; Tapper, J.; Pere, H.; El-Rafai, W.; Hemmer, S.; Wasenius, V.-M.; Vidgren, V.; Zhu, Y. *Am. J. Path.* **1998**, *152*, 1107.

[7] Laird, A. D.; Cherrington, J. M. *Expert. Opin. Investig. Drugs* **2003**, *12*, 51.

[8] Kumar, C. C.; Madison, V. *Expert. Opin. Emerging Drugs* **2001**, *6*, 303.

[9] Knighton, D. R.; Zheng, J. H.; Ten Eyck, L. F.; Ashford, V. A.; Xuoung, N. H.; Taylor, S. S.; Sowadski, J. M. *Science* **1991**, *253*, 407.

[10] Knighton, D. R.; Zheng, J. H.; Ten Eyck, L. F.; Xuoung, N. H.; Taylor, S. S.; Sowadski, J. M. *Science* **1991**, *253*, 414.

[11] Zheng, J. H.; Trafney, E. A.; Knighton, D. R.; Xuoung, N. H.; Taylor, S. S.; Ten Eyck, L. F.; Sowadski, J. M. *Acta Crystallogr.* **1993**, *D49*, 362.

[12] Zheng, J. H.; Knighton, D. R.; Ten Eyck, L. F.; Karlsson, R.; Xuoung, N. H.; Taylor, S. S.; Sowadski, J. M. *Biochemistry* **1993**, *32*, 2154.

[13] Yamaguchi, H.; Hendrickson, W. A. *Nature* **1996**, *384*, 484.

[14] Lisnock, J.-M.; Tebben, A.; Frantz, B.; O'Neill, E. A.; Croft, G.; O'Keefe, S. J.; Li, B.; Hacker, C.; de Laszlo, S.; Smith, A.; Libby, B.; Liverton, N.; Hermes, J.; LoGrasso, P. *Biochemistry* **1998**, *37*, 16573.

[15] Hubbard, S. R.; Till, J. H. *Annu. Rev. Biochem.* **2000**, *69*, 373.

[16] ter Haar, E.; Col, J. T.; Austen, D. A.; Hsiao, H.-M.; Swenson, L.; Jain, J. *Nat. Struc. Biol.* **2001**, *8*, 593.

[17] Brown, N. R.; Noble, M. E.; Endicott, J. A.; Johnson, L. N. *Nat. Cell Biol.* **1999**, *1*, 438.

[18] Wilson, K. P.; McCaffrey, P. G.; Hsiao, K.; Pazhanisamy, S.; Galullo, V.; Bemis, G. W.; Fitzgibbon, M. J.; Caron, P. R.; Murcko, M. A.; Su, M. S. *Chem. Biol* **1997**, *4*, 423.

[19] Robinson, M. J.; Harkins, P. C.; Zhang, J.; Baer, R.; Haycock, J. W.; Cobb, M. H.; Goldsmith, E. J. *Biochemistry* **1996**, *35*, 5641.

[20] Canagarajah, B. J.; Khokhlatchev, A.; Cobb, M. H.; Goldsmith, E. J. *Cell* **1997**, *90*, 859.

[21] Bellon, S.; Fitzgibbon, M. J.; Fox, T.; Hsiao, H. M.; Wilson, K. P. *Struc. Fold. Des.* **1999**, *7*, 1057.

[22] Schindler, T.; Sicheri, F.; Pico, A.; Gazit, A.; Levitski, A.; Kuriyan, J. *Mol. Cell* **1999**, *3*, 639.

[23] Mohammedi, M.; Froum, S.; Hamby, J. M.; Schroeder, M. C.; Panek, R. L.; Liu, G. H.; Eliseenkova, A. V.; Green, D.; Schlessinger, J.; Hubbard, S. R. *EMBO J.* **1998**, *17*, 5896.

[24] Schindler, T.; Bornmann, W.; Pellicena, P.; Miller, W. T.; Clarkson, B.; Kuriyan, J. *Science* **2000**, *289*, 1938.

[25] Nagar, B.; Bornmann, W.; Pellicena, P.; Schindler, T.; Veach, D.; Miller, W.; Clarkson, B.; Kuriyan, J. *Cancer Res* **2002**, *62*, 4236.

[26] Macdonald, S. J. F.; Smith, P. W. *Drug Disc. Today* **2001**, *6*, 947.

[27] Ramesha, C. S. *Drug Disc. Today* **2000**, *5*, 43.

[28] Michne, W. F. *Pharma. News* **1996**, *3*, 19.

[29] Kenny, B. A.; Bushfield, M.; Parry-Smith, D. J.; Fogarty, S.; Treherne, J. M. *Prog. Drug Res.* **1998**, *51*, 245.

[30] Broach, J. R.; Thorner, J. *Nature* **1996**, *384*, 14.

[31] Labaudiniere, R. F. *Drug Discov. Today* **1998**, *3*, 511.

[32] Walters, W. P.; Murcko, M. A. *Advanced Drug Delivery Reviews* **2002**, *54*, 255.

[33] Walters, W. P.; Ajay; Murcko, M. A. *Curr. Opin. Chem. Biol.* **1999**, *3*, 384.

[34] Clark, D. E.; Pickett, S. D. *Drug Disc. Today* **2000**, *5*, 49.

[35] Lipinski, C. A.; Lombardo, F.; Dominy, B. W.; Feeney, P. J. *Adv. Drug Deliv. Rev.* **1997**, *23*, 3.

[36] Spencer, R. W. *Biotechnology and Bioengineering* **1998**, *61*, 61.

[37] Walters, W. P.; Namchuk, M. N. *Nat. Rev. Drug Disc.* **2003**, *2*, 259.

[38] Muegge, I.; Rarey, M. In *Reviews in Computational Chemistry, Volume 17*; Lipkowitz, K. B.; Boyd, D. B. Eds.; Wiley: New York, NY, **2001**; pp 1.

[39] Boehm, H.-J.; Stahl, M. In *Reviews in Computational Chemistry,* Volume *18*; Lipkowitz, K. B., Boyd, D. B., Eds.; Wiley: New York, NY, **2002**; pp 41.

[40] Charifson, P. S.; Corkery, J. J.; Murcko, M. A.; Walters, W. P. *J. Med. Chem.* **1999**, *42*, 5100.

[41] Sheridan, R. P.; Kearsley, S. K. *Drug Discov. Today* **2002**, *7*, 903.

[42] Nilakantan, R.; Bauman, N.; Dixon, J. S.; Venkataraghavan, R. *J. Chem. Inf. Comput. Sci.* **1986**, *27*, 82.

[43] Carhart, R. E.; Smith, D. H.; Venkataraghavan, R. *J. Chem. Inf. Comput. Sci.* **1984**, *25*, 64.

[44] Willett, P.; Barnard, J. M.; Downs, G. M. *J. Chem. Inf. Comput. Sci.* **1998**, *38*, 983.

[45] Good, A. C.; Mason, J. S. In *Reviews in Computational Chemistry, Volume 7*; Lipkowitz, K. B.; Boyd, D. B. Eds.; Wiley: New York, NY, 1995; pp 67.

[46] Agrafiotis, D. K.; Myslik, J. C.; Salemme, F. R. *Molecular Diversity* **1998**, *4*, 1.

[47] Kier, L. B.; Hall, L. H. *Molecular Structure Description: The Electrotopological State*; Academic Press: New York, NY, **1999**.

[48] Oprea, T. I. *Curr. Opin. Chem. Biol.* **2002**, *6*, 384.

[49] Pearlman, R. S.; Smith, K. M. *J. Chem. Inf. Comput. Sci.* **1999**, *39*, 28.

[50] Bemis, G. W.; Murcko, M. A. *J. Med. Chem.* **1996**, *39*, 2887.

[51] Landro, J. A.; Taylor, I. C. A.; Stirtan, W. G.; Osterman, D. G.; Kristie, J.; Hunnicutt, E. J.; Rae, P. M. M.; Sweetman, P. M. . *J. Pharmacol. Toxicol. Methods* **2000**, *44*, 273.

[52] McGovern, S. L.; Caselli, E.; Grigorieff, N.; Shoichet, B. K. *J. Med. Chem.* **2002**, *45*, 1712.

[53] Namchuk, M. N. *Targets* **2002**, *1*, 125.

[54] Davies, S. P.; Reddy, H.; Caivano, M.; Cohen, P. *Biochem. J.* **2000**, *351*, 95.

[55] Hanke, J. H.; Gardner, J. P.; Dow, R. L.; Changelian, P. S.; Brissette, W. H.; Weringer, E. J.; Pollok, B. A.; Connelly, P. A. *J. Biol. Chem.* **1996**, *271*, 695.

[56] Tatton, L.; Morley, G. M.; Chopra, R.; Khwaja, A. *J. Biol. Chem.* **2003**, *278*, 4847.

[57] Parker, G. J.; Law, L. L.; Lenoch, F. J.; Bolger, R. E. *J. Biomol. Screening* **2000**, *5*, 77.

[58] Sills, M. A.; Weiss, D.; Pham, Q.; Schweitzer, R.; Wu, X.; Wu, J. J. *J. Biomol. Screening* **2002**, *7*, 191.

[59] Cook, P. F.; Neville Jr., M. E.; Vrana, K. E.; Hartl, T.; Roskoski Jr., R. *Biochemistry* **1982**, *21*, 5794.

[60] Kauvar, L. M.; Higgins, D. L.; Villar, H. O.; Sportsman, J. R.; Engqvist-Goldstein, A.; Bukar, R.; Bauer, K. E.; Dilley, H.; Rocke, D. M. *Chem. Biol.* **1995**, *2*, 107.

[61] Frye, S. V. *Chem. Biol.* **1999**, *6*, R3.

[62] Fox, T.; Coll, J. T.; Xie, X.; Ford, P. J.; Germann, U. A.; Porter, M. D.; Pazhanisamy, S.; Fleming, M. A.; Galullo, V.; Su, M. S.; Wilson, K. P. *Protein Sci.* **1998**, *7*, 2249.

[63] Bohmer, F. D.; Karagyozov, L.; Uecker, A.; Serve, H.; Botzki, A.; Mahboobi, S.; Dove, S. **2003**, *278*, 5148.

[64] Badger, A. M.; Bradbeer, J. N.; Votta, B.; Lee, J. C.; Adams, J. L.; Griswold, D. E. *J. Pharmacol. Exp. Ther.* **1996**, *279*, 1453.

[65] Dinarello, C. A. *Curr. Opin. Immunol.* **1991**, *3*, 941.
[66] Dinarello, C. A. *Blood* **1996**, *87*, 2095.
[67] Tracey, K. J.; Cerami, A. *Annu Rev Med* **1994**, *45*, 491.
[68] Jarvis, B.; Faulds, D. *Drugs* **1999**, *57*, 945.
[69] Garrison, L.; McDonnell, N. D. *Ann. Rheum. Dis.* **1999**, *58* (Suppl. 1), 65.
[70] Maini, R.; Clair, E. W.; Breedveld, F.; Furst, D.; Kalden, J.; Weisman, M.; Smolenm\, J.; Emery, P.; Harriman, G.; Feldmann, M.; Lipsky, P. *Lancet* **1999**, *354*, 1932.
[71] Present, D. H.; Rutgeerts, P.; Targan, S.; Hanauer, S. B.; Mayer, L.; van Hogezand, R. A.; Podolsky, D. K.; Sands, B. E.; Braakman, T.; DeWoody, K. L.; Schaible, T. F.; van Deventer, S. J. *N. Eng. J. Med.* **1999**, *340*, 1398.
[72] Rutgeerts, P. *Aliment. Pharmacol. Ther.* **1999**, *13* (Suppl. 4), 9.
[73] Lee, J. C.; Laydon, J. T.; McDonnell, P. C.; Gallagher, T. F.; Kumar, S.; Green, D.; McNulty, D.; Blumenthal, M. J.; Heys, J. R.; Landvatter, S. W.; et al. *Nature* **1994**, *372*, 739.
[74] Lechner, C.; Zahalka, M. A.; Giot, J. F.; Moller, N. P.; Ullrich, A. *Proc Natl Acad Sci USA* **1996**, *93*, 4355.
[75] Jiang, Y.; Gram, H.; Zhao, M.; New, L.; Gu, J.; Feng, L.; Di Padova, F.; Ulevitch, R. J.; Han, J. *J. Biol. Chem.* **1997**, *272*, 30122.
[76] Cuenda, A.; Rouse, J.; Doza, Y. N.; Meier, R.; Cohen, P.; Gallagher, T. F.; Young, P. R.; Lee, J. C. *FEBS Lett.* **1995**, *364*, 229.
[77] Salituro, F. G.; Bemis, G. W.; Germann, U. A.; Duffy, J. P.; Galullo, V. P.; Harrington, E. M.; Pazhanisamy, S.; Ford, P. J.; Cepek, K. L.; Wang, Y.-M. C.; Bellon, S. F.; Ku, G.; Wilson, K. P.; Su, M. S.-S. In *XXXVIIemes Rencontres Internationales de Chimie Therapeutique*; Elsevier: Tours, France, **2001**; Vol. *28*, pp 173.
[78] Hanks, S. K.; Quinn, A. M. *Methods Enzymol.* **1991**, *200*, 38.
[79] Salituro, F.; Galullo, V.; Bellon, S.; Bemis, G. W.; Cochran, J. In *WO99/58502*, **1999**.
[80] Irving, E. A.; Barone, F. C.; Reith, A. D.; Hadingham, S. J.; Parsons, A. A. *Brain Res. Mol. Brain Res.* **2000**, *77*, 65.
[81] Hayashi, T.; Sakai, K.; Sasaki, C.; Zhang, W. R.; Warita, H.; Abe, K. *Neurosci. Lett.* **2000**, *284*, 195.
[82] Barone, F. C.; Parsons, A. A. *Exp. Opin. Invest. Drugs* **2000**, *9*, 2281.
[83] Fejzo, J.; Lepre, C. A.; Peng, J. W.; Bemis, G. W.; Ajay; Murcko, M. A.; Moore, J. M. *Chemistry & Biology* **1999**, *6*, 755.
[84] Lepre, C. A.; Peng, J.; Fejzo, J.; Abdul-Manan, N.; Pocas, J.; Jacobs, M.; Xie, X.; Moore, J. M. *Comb. Chem. High Throughput Screen.* **2002**, *5*, 583.
[85] Sinha, S.; Corey, S. J. *J. Hematotherapy Stem Cell Res.* **1999**, *8*, 465.
[86] Bolen, J. B.; Brugge, J. S. *Annu. Rev. Immunol.* **1997**, *15*, 371.
[87] Green, J.; Bemis, G. W.; Grillot, A.-L.; Ledeboer, M.; Salituro, F.; Harrington, E. M.; Gao, H.; Baker, C.; Cao, J.; Hale, M. In *WO0112621*; Vertex Pharmaceuticals Incorporated, **2001**.
[88] Parang, K.; Till, J. H.; Ablooglu, A. J.; Kohanski, R. A.; Hubbard, S. R.; Cole, P. A. *Nat. Struc. Biol.* **2001**, *8*, 37.
[89] Favelyukis, S.; Till, J. H.; Hubbard, S. R.; Miller, W. T. *Nat. Struc. Biol.* **2001**, *8*, 1058.
[90] Stamos, J.; Sliwkowski, M. X.; Eigenbrot, C. *J. Biol. Chem.* **2002**, *277*, 46265.
[91] Mohammadi, M.; McMahon, G.; Sun, L.; Tang, C.; Hirth, P.; Yeh, B. K.; Hubbard, S. R.; Schlessinger, J. *Science* **1997**, *276*, 955.
[92] Wybenga-Groot, L. E.; Baskin, B.; Ong, S. H.; Tong, J.; Pawson, T.; Sicheri, F. *Cell* **2001**, *106*, 745.
[93] Xu, W.; Doshi, A.; Lei, M.; Eck, M. J.; Harrison, S. C. *Cell* **1999**, *3*, 629.
[94] Sicheri, F.; Moarefi, I.; Kuriyan, J. *Nature* **1997**, *385*, 602.
[95] Mao, C.; Zhou, M.; Uckun, F. M. *J. Biol. Chem.* **2001**, *276*.
[96] Lamers, M. B. A. C.; Antson, A. A.; Hubbard, R. E.; Scott, R. K.; Williams, D. H. *J. Mol. Biol.* **1999**, *285*, 713.
[97] Wilson, K. P.; Fitzgibbon, M. J.; Caron, P. R.; Griffith, J. P.; Chen, W.; McCaffrey, P. G.; Chambers, S. P.; Su, M. S. *J. Biol. Chem.* **1996**, *271*, 27696.
[98] Xie, X.; Gu, Y.; Fox, T.; Coll, J. T.; Fleming, M. A.; Markland, W.; Caron, P. R.; Wilson, K. P.; Su, M. S. *Structure* **1998**, *6*, 983.
[99] Kimble, R. B.; Matayoshi, A. B.; Yannice, J. L.; Kung, V. T.; Williams, C.; Pacifici, R. *Endocrinology* **1995**, *136*, 3054.